energies

MDPI

Review

Hydrogen Carriers: Scientific Limits and Challenges for the Supply Chain, and Key Factors for Techno-Economic Analysis

Davide Clematis [1,*], Daria Bellotti [2], Massimo Rivarolo [2], Loredana Magistri [2] and Antonio Barbucci [1,3]

[1] Department of Civil, Chemical and Environmental Engineering, University of Genoa, Via All'Opera Pia 15, 16145 Genoa, Italy; barbucci@unige.it
[2] Thermochemical Power Group, DIME, University of Genoa, Via Montallegro 1, 16145 Genoa, Italy; daria.bellotti@unige.it (D.B.); massimo.rivarolo@unige.it (M.R.); magistri@unige.it (L.M.)
[3] Institute of Condensed Matter Chemistry and Technology for Energy, National Research Council (CNR-ICMATE), Via de Marini 6, 16149 Genoa, Italy
* Correspondence: davide.clematis@unige.it

Abstract: Hydrogen carriers are one of the keys to the success of using hydrogen as an energy vector. Indeed, sustainable hydrogen production exploits the excess of renewable energy sources, after which temporary storage is required. The conventional approaches to hydrogen storage and transport are compressed hydrogen (CH_2) and liquefied hydrogen (LH_2), which require severe operating conditions related to pressure (300–700 bar) and temperature (T < −252 °C), respectively. To overcome these issues, which have hindered market penetration, several alternatives have been proposed in the last few decades. In this review, the most promising hydrogen carriers (ammonia, methanol, liquid organic hydrogen carriers, and metal hydrides) have been considered, and the main stages of their supply chain (production, storage, transportation, H_2 release, and their recyclability) have been described and critically analyzed, focusing on the latest results available in the literature, the highlighting of which is our current concern. The last section reviews recent techno-economic analyses to drive the selection of hydrogen carrier systems and the main constraints that must be considered. The analyzed results show how the selection of H_2 carriers is a multiparametric function, and it depends on technological factors as well as international policies and regulations.

Keywords: hydrogen carrier; compressed hydrogen; liquefied hydrogen; ammonia; methanol; LOHC; formic acid; metal hydride; techno-economic analysis; hydrogen storage

Citation: Clematis, D.; Bellotti, D.; Rivarolo, M.; Magistri, L.; Barbucci, A. Hydrogen Carriers: Scientific Limits and Challenges for the Supply Chain, and Key Factors for Techno-Economic Analysis. *Energies* **2023**, *16*, 6035. https://doi.org/10.3390/en16166035

Academic Editor: Vladislav A. Sadykov

Received: 31 July 2023
Revised: 12 August 2023
Accepted: 14 August 2023
Published: 17 August 2023

1. Introduction

Hydrogen is an attractive energy vector due to its high gravimetric energy density (e.g., 120 MJ/kg_{H2} vs. 55.6 MJ/kg_{CH4} for methane), and the potentiality to make power production carbon-neutral. Nevertheless, its production is still highly dependent on fossil fuels and only 4% is derived from water electrolysis [1], and so relevant efforts are required in making hydrogen an energy carrier suitable for a sustainable green economy. In the last decades, researchers have focused on several kinds of water electrolyzers, such as polymer electrolytes membrane (PEMWEs) [2,3], alkaline water electrolyzers (AWE) [4,5], and solid oxide electrolyzers cells (SOEC) [6,7], which differ in component materials and operating conditions. Moreover, in green hydrogen production, electrolyzers must exploit the excess energy from the renewable energy sources (RES) grid, and then, in a reasonable scenario, hydrogen is not immediately used when produced, and so storage systems are required [8–13]. The hydrogen storage systems must display key features to be competitive with conventional fuels (gasoline, methane, liquid natural gas) and other energy storage systems (batteries). They must provide high safety standards, allow fast hydrogen release when required, and be economically sustainable. Moreover, with hydrogen being the lightest element, it has the intrinsic limitation of a low volumetric energy density under ambient conditions, thus introducing storage and transport issues.

Currently, the most common method of hydrogen storage is to pressurize the gas in high-pressure tanks (350–700 bar) [14,15]. The high pressure has the benefit of reducing the volume required, but the compression work required has a negative impact on the global energy balance, with a consumption equivalent to 11–13% of the energy contained in the stored H_2 [16]. In addition, other technological issues are still unsolved, limiting the application of such an approach. The severe operating pressure places strong mechanical stress on the vessels, which are mainly made of steel or aluminium. As such, the shell must have a thickness able to tolerate the tension and meet safety requirements not only under conventional operating conditions, but also during undesirable events such as collisions [17]. The direct consequence is an increase in the weight of the hydrogen vessel, which strongly impacts the suitability of this methodology for mobile applications. Furthermore, molecular hydrogen can cause serious damage to infrastructure (metal tanks and pipelines) due to the activation of phenomena such as H_2 embrittlement, which reduces the lifetime service of the structure itself [18,19]. Alternative materials such as carbon fiber reinforcements have been investigated for lighter vessels, preserving mechanical resistance, but despite the promising results, the material costs limit large-scale applications. Nevertheless, hydrogen storage at high pressures could be interesting for stationary applications, and for creating "hydrogen banks" able to store a high volume of hydrogen. This concept would exploit the possibility of storing an elevated amount of hydrogen in salt caverns. These are particularly favorable for this area due to their low permeability to H_2, thus reducing gas leakages [20,21].

Hydrogen can be also stored in a liquid state, but this requires extremely low temperatures (−253 °C), which can be reached only by high energy-consuming cryogenic loops [22–24]. The keeping of such low temperatures consumes at least 30% of the stored energy, thus decreasing global efficiency [25,26]. On the other side, liquid storage operates at a lower pressure than gaseous, reducing the vessel weight and improving safety conditions. Nevertheless, the costs are still too high for widespread usage, and this method is suitable only for niche applications where the release of hydrogen occurs in a short time, based on relevant investments.

Lately, other alternatives have been developed for hydrogen storage; among them, liquid carriers such as ammonia [27–29], methanol [30–32] and formic acid [33,34], as well as systems based on more complex liquid organic hydrogen carriers (LOHC) [35–37] or solid materials such as metal hydrides, could play a relevant role in the near future. The interest in alternative hydrogen carriers has increased due to the possibility of their operating in milder conditions (pressure and temperature) than those required by CH_2 and LH_2. In these systems, hydrogen is stored by means of the formation of bonds, as a result of which the sustainability of all stages of the supply chain must be considered. Indeed, despite the promising results already reported in the literature, this review shows that several issues still arise, hindering their application at a large scale.

In this review, the main features of the above-mentioned hydrogen carriers have been considered, focusing on their production, transport, and final hydrogen release, highlighting for each of them the main challenges that must be faced in order to reach full application and deep market penetration. In the last section, a thermo-economic comparison is proposed based on the literature, highlighting the key factors that must be considered for the selection of the most suitable technology.

2. Hydrogen Carriers Supply Chain: From Production to Hydrogen Release

In the last two decades, several alternatives have been proposed to overcome the severe conditions required to employ CH_2 and LH_2 technologies. The most promising approaches discussed in the following sections are based on the storage of hydrogen through the formation of chemical bonds in a more complex molecule: the hydrogen carrier. In Table 1, key physical features of the hydrogen carriers discussed in the next section are compared with hydrogen and methane. In this review, methane is not closely discussed as a next-generation hydrogen carrier, despite its large usage and the role that

it can play during the current energy transition. Although the CO_2 methanation reaction allows for the storage of hydrogen in methane by exploiting captured carbon dioxide, and it shows full compatibility with the energy infrastructure, methane storage requires severe conditions relating to temperature or pressure due to the physical properties of methane (boiling temperature −161.5 °C, volumetric energy density at ambient pressure 0.0378 MJ/L). Such intrinsic limitations have already been raised for pure hydrogen storage, and high-pressure or cryogenic loops are used as they are competitive with other possible energy vectors. These two approaches have a negative impact on process energy balance, justifying the interest in the development of energy carriers that can store hydrogen under milder conditions.

Table 1. Main physical characteristics of hydrogen, methane, and hydrogen carriers considered in this review.

Carrier	Boling Temperature (°C)	Flash Point Temperature (°C)	Inflammability Range (Vol%)	H_2 Capacity (wt. %)	Volumetric Energy Density (MJ/L)
Hydrogen	−252.9	Flammable gas	4–75%	100	0.0107 (amb. pressure) 2.757 (CH_2 @ 350 bar) 4.712 (CH_2 @ 700 bar) 8.506 (LH_2 @ −253 °C)
Methane	−161.5	−188	4.4–17%	25	0.0378 (amb. pressure) 5.800 (150 bar) 9.200 (250 bar) 22.200 (−163 °C, 1 bar)
Ammonia	−33.4	/	15–33.6%	17.8	12.700 (10 bar, −34 °C)
Methanol	64.7	9.9	6–50%	12.5	15.8
Formic Acid	100.8	69	18–51%	4.3	7.2
Benzene Cyclohexane	80 81	−11 −18	1.2–8% 1.3–8.4%	7.2	6.660
Toluene Methylcyclohexane	111 101	4 −6	1.1–7.1% 1.2–6.7%	6.2	5.640
Naphthalene Decalin	218 185	80 57	0.9–5.9% 0.7–5.4%	7.3	7.777
Dibenzyltoluene Perhydrodibenzyltoluene	390 287	212	/	6.2	6.786
$NaBH_4$	/	/	/	10.8	15.48
MgH_2	/	/	/	7.6	15.84

Independent of its chemical composition, a suitable hydrogen carrier must provide:

- A sufficient hydrogen capacity (>5 wt. %);
- Easy and environmentally friendly production process;
- Not too harsh conditions and high stability during storage;
- Easy and safe handling during transport;
- Low energy consumption during hydrogen release;
- Option to be recycled.

This list identifies the main features that characterize the supply chain of hydrogen carriers: production, storage and transport, and hydrogen release for final utilization. In the following sections, all these stages, sketched in Figure 1, will be discussed for the hydrogen carriers considered in this review. At the end of this section, Table 2 summarizes the main challenges for each hydrogen carrier analyzed.

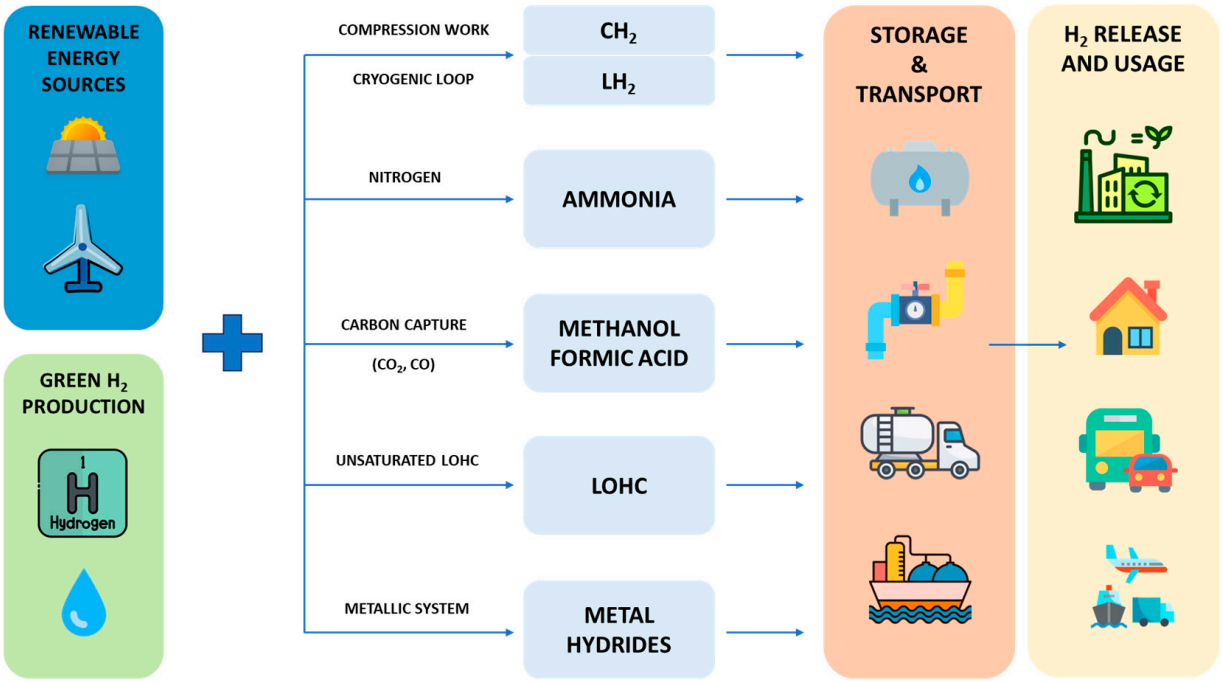

Figure 1. Schematic representation of the supply chain for hydrogen storage and carriers considered in this review.

Table 2. Current challenges for hydrogen carriers considered in this review.

Hydrogen Carrier	Current Challenges for Next Studies
Ammonia	• Development of catalytic systems able to operate at lower temperatures and pressure than the Haber–Bosch process. • Decrease the content of critical raw materials (CRM) and PGM elements in catalyst formulation. • Development of alternative processes for ammonia synthesis (e.g., electrochemical synthesis). • Increase the kinetics of ammonia cracking under milder operating conditions.
Methanol	• Integration of methanol synthesis with CCS technologies for reducing environmental impact. • Boost the research on the electrochemical process for methanol synthesis. • Decrease the amount of PGM elements in the catalyst for methanol cracking. • Improve catalyst selectivity in both the hydrogenation and dehydrogenation process.
Formic Acid	• Improve the activity and the selectivity of heterogeneous catalysis for formic acid synthesis. • Identification of green organic solvents for formic acid synthesis in liquid-state processes. • Optimization of heterogeneous catalyst architecture for formic acid dehydrogenation.
Liquid Organic Hydrogen Carriers	• Replacement of Pt-based catalysts for hydrogenation and dehydrogenation. • Improve catalyst tolerance towards wet hydrogen and impurities. • Improve dehydrogenation kinetic at milder conditions. • Improve recyclability service life by enhancing the selectivity of the dehydrogenation process towards the desired unsaturated LOHC.
Metal Hydrides	• Development of a simpler process for hydrogen storage. • Improve recyclability of metal hydride (>1500 cycles). • Improve hydrogen release under milder conditions (T < 85 °C).

2.1. Ammonia

2.1.1. Ammonia Production

Ammonia is one of the most widely produced chemicals, with worldwide production, and it has an attractive hydrogen content of 17.6 wt. %. Today 96% of the commercialized NH_3 is synthesized by the Haber–Bosch process, developed in the early 1900s [27,38]. In this well-established industrial process, nitrogen (N_2) and hydrogen (H_2) react on magnetite (Fe_3O_4) used as a heterogeneous catalyst:

$$N_{2(g)} + 3H_{2(g)} \rightleftarrows 2NH_{3(g)} \quad (1)$$

The weakly exothermic reaction (−92.4 kJ/mol) is usually carried out in temperature and pressure ranges of 350–550 °C and 150–320 atm, respectively, to shift the equilibrium towards the product. Despite the depth of knowledge regarding its synthesis and worldwide utilization, the greenhouse gases (GHG) associated with the Haber–Bosch process are high, accounting for 1.2% of the total GHG emissions [27]. Furthermore, the production pathway and its environmental impact are key factors that make ammonia a valuable hydrogen carrier. In this context, three possible approaches can be followed. The first action deals with hydrogen production, which up to now has been based on methane, natural gas, oil, and coal. This stage must be shifted to technologies based on water electrolysis powered by RES, with a drastic reduction in GHG. The second action is focused on the development of catalysts able to provide a significant industrial application under milder conditions, reducing the overall energy consumption, while the third is the aspiration towards a revolution in process design, with alternative approaches for the synthesis of NH_3.

H_2 production by water electrolysis is beyond the scope of this review, but updated discussions about electrolyzers can be found here [9,39,40]. Focusing on the catalysts used for ammonia synthesis, nowadays, the research is oriented towards material with a significant catalytic activity at lower temperatures and pressure than the state-of-the-art catalysts, and they must be economically sustainable. Several catalyst formulations have been proposed, and the most promising materials are based on iron (Fe), ruthenium (Ru), cobalt (Co), and nickel (Ni) [41,42]. As previously introduced, Fe-based catalysts represent the reference for ammonia synthesis, and their compositions are similar to those proposed by Bosch. The commercial catalyst has Fe_3O_4 as its main active phase, with the small addition of oxides used as promoters and stabilizers such as Al_2O_3 (2.5 wt. %), CaO (2.0 wt. %), K_2O (0.8 wt. %), SiO_2 (0.4 wt. %), MgO (0.3 wt. %), and traces of TiO_2, ZrO_2, and V_2O_5, with a maximum service-life of 10 years [43]. The deactivation is mainly due to the sintering between iron particles, enhanced by the formation of local hotspots. Moreover, in the conventional Haber–Bosch process, where the H_2 used for ammonia production is derived from methane steam reforming, the presence of oxygenated compounds (CO, CO_2, O_2, H_2O) can produce surface poisoning. This is reversible if the exposition is limited to a few weeks, but becoming irreversible if extended over time. Irreversible poisoning is also induced by the presence of chlorinated and sulfur compounds [44].

Another class of catalysts already used at the industrial scale is based on Ru, such as in the Kellogg process. The higher catalytic activity of Ru than conventional Fe-based catalysts allows for a decrease in operating conditions (pressure and temperature). Considering that ruthenium belongs to PGM, it is mainly used as the supporting phase on a cheaper material for the sake of cost reduction. Indeed, the elevated cost is one of the key factors that hinders its utilization as the main catalyst for industrial applications. Moreover, the literature shows that, despite the promising catalytic activity, Ru-based catalysts suffer from the presence of oxygen, as discussed for Fe-based catalysts, with fast deactivation, as reported by [45].

To overcome the price issues related to ruthenium, other elements such as cobalt and nickel have been considered as possible candidates for NH_3 production. For these elements, the catalytic activity can be improved using promoters. In 2022, Gao et al. [46] reported that barium hydride (BaH_2) can have a synergic effect with Ni, with a drastic

reduction in the activation energy from 150 kJ mol^{-1} (bare Ni-Mg-O catalyst) to 87 kJ mol^{-1}, enhancing nitrogen hydrogenation. Previously (2021), Sato et al. [47] also identified barium has an element for boosting the activity of Co-based catalysts. They found that a simple encapsulation of Co nanoparticles supported on MgO with BaO leads to an increase in the NH_3 synthesis rate to up to 80 times higher than that obtained without barium addition. The presence of BaO, which facilitates strong electro-donation to Co surface atoms, decreases the energy for the N≡N cleavage bond. It is noteworthy that the proposed catalyst formulation also maintains promising activity under milder conditions (150 °C, 10 bar), proffering the development of less energy-consuming processes.

Alternative approaches proposed for ammonia synthesis are based on electrochemical cells with different systems that can operate in a wide temperature range. High-temperature systems (T > 400 °C) are based on solid-state electrolytes (protonic or anionic), and N_2 and H_2 are fed to the electrodes. The operating temperature is linked to the ionic conductivity of the electrolyte and the catalytic activity of electrodes. Although systems operating at over 600 °C have been proposed to increase the sluggish kinetics, most of the works are oriented towards temperatures lower than 600 °C [42] for reducing operating costs. At higher temperatures, yttrium and cerium are considered the main elements for electrolyte formulation. At lower temperatures (400–450 °C), carbonate-based materials have been proposed, using Ag–Pd-based electrodes [48]. Nevertheless, the energy consumption associated with this process and the low Faradaic Efficiency (FE) make this approach unsuitable for competing with conventional ammonia processes, and further investigations and improvements are required.

An attempt to decrease the energy demand has been made via the lowering of operating temperatures to below 100 °C. The low-temperature electrochemical process for ammonia synthesis is usually carried out in a basic solution (KOH) using a proton-conducting membrane (e.g., Nafion®). Common electrodes are made up of Pt (anode) and Ru (cathode), and the utilization of Pt affects the purity required for water/hydrogen in the inlet stream. This cell setup leads to a production rate of 2×10^{-11} mol s^{-1} cm^{-2} at 90 °C with FE below 1%. A relevant improvement in production rate and current efficiency (1.13×10^{-8} mol s^{-1} cm^{-2} at 80 °C, with current efficiency of 90%) has been obtained with an anode and cathode made up Ni–$Sm_{0.2}Ce_{0.8}O_{2-\delta}$ and $SmFe_{0.7}Cu_{0.3-x}Ni_xO_3$, respectively, highlighting the possibility of achieving interesting performance, and the current necessity to investigate new electrode systems [49].

Another electrochemical path recently proposed for distributed ammonia production is based on the electrochemical reduction of nitrogen species, such as nitrates (NO_3^-), nitrites (NO_2^-) and nitric oxide (NO) [50]. These processes have the advantages that the double bond between nitrogen and oxygen is characterized by lower energy (204 kJ mol^{-1}) compared to the triple bond of N_2 (941 kJ mol^{-1}), making the exploitation of these species more interesting [50]. The efforts made to develop such electrochemical systems are also justified by considering a circular economy view. Indeed, these ions are detected in wastewater (NO_3^-, NO_2^-) from agricultural and industrial sites, and NO is mainly present in waste gases. Their presence in water or air represents a risk for both the environment and human health [51,52], necessitating their removal. Based on these aspects, a proper design of wastewater and flue gas treatments allows for obtaining a concentrated nitrogenous stream that can be used as feed for the electrochemical process. Figure 2 summarizes the main reaction path characteristic of ammonia production based on NO_2^-, NO_3^- and NO. The key steps of the reaction involve the adsorption of the reactant on the cathode surface, followed by an electron and proton transfer. It is important to keep in mind that the limiting stage changes as a function of the starting nitrogenous species, with consequences for electrocatalysts development.

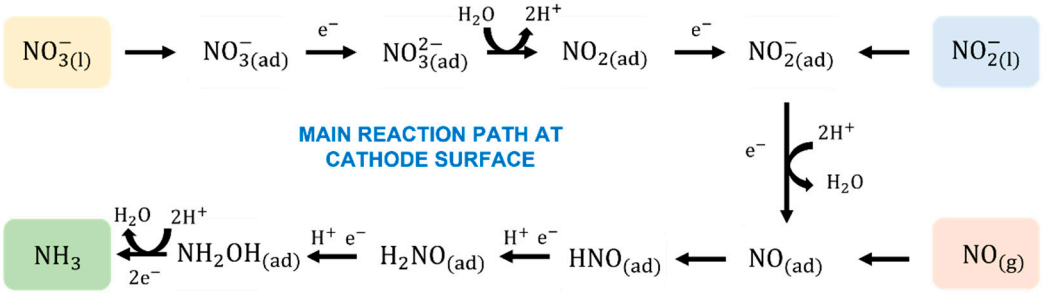

Figure 2. Main reaction path for nitrogen species reduction at the cathode surface. Figure adapted from [50].

NO_3^- is probably the most appealing nitrogen ion, due to its diffuse presence in water (wastewater, surface water, groundwater). Based on the literature, the first reduction stage of NO_3^- to NO_3^{2-} is the limiting step of the kinetic mechanism. For industrial applications, it is necessary to increase the NO_3^- concentration close to the cathode surface, to improve Faradaic Efficiency (FE) and limit the competitive hydrogen evolution reaction (HER). The simplest approach uses selective membranes to form a high-NO_3^- catholyte environment, but the most update studies look for double-purpose cathode materials [50]. In this view, the electrode provides both a high adsorption capacity and high electrocatalytic properties for NO_3^-. The high adsorption rate locally increases the NO_3^- concentration, supporting a higher FE. Carbonaceous porous structures have been recently investigated due to their elevated adsorption properties, and the functionalization of their surface with metals, such as copper, further allows for ammonia synthesis at low nitrate concentrations [53]. Other promising adsorbents include carbon nanotubes (CNTs) activated with polyaniline and cobalt oxide (Co_3O_4) [54]. The presence of polyaniline makes the system more selective towards NO_3^- adsorption, with a local increase in its concentration at the cathode surface, and the Co_3O_4 supplies electrocatalytic activity for its reduction to ammonia.

When NO_2^- is the main nitrogen source, the key aspect that must be considered in electrocatalyst design is the high production of H^* and the simultaneous limitation of the hydrogen evolution. The most promising systems for sustaining this reaction are made up of metal nanoparticles (e.g., Ru, Cu) distributed on carbon-based supports (e.g., carbon nitride) [55].

Nitrogen oxide is mainly formed during the combustion process, after which it is present in the atmosphere. The reduction of NO to its liquid phase is strictly limited by its low solubility. The strategies currently under development for increasing performances are the usage of gas diffusion electrodes [56] or solid electrolyte cells working at high temperatures [57]. Nevertheless, all these technologies used for ammonia production from nitrogen oxide and ions are still far from operability at the industrial scale, and further efforts will be necessary in the near future.

2.1.2. Hydrogen Release from Ammonia

Among the ensuing stages of supplying ammonia as a hydrogen carrier, hydrogen release is the most challenging. Indeed, despite the fact that the storage and transport of NH_3 is based on a deep and widespread knowledge base, ammonia decomposition is still facing issues that impact the process' sustainability [58]. The reaction is thermodynamically favored over 400 °C, but the kinetics are limited by the high activation energy of N–H blond cleavage and molecular nitrogen desorption. For these reasons, the current research is looking for catalysts active at reasonably non-severe conditions, tuning their composition and morphology, and the interactions between the active phase/support. Theoretically, the catalytic systems used for ammonia synthesis should also be able to support the decomposition reaction; nevertheless, the results clearly show the necessity of developing tailored materials for process optimization, due to the different reaction pathways [58]. Promising active catalysts are usually made of alloys between noble metals (Ir, Rh, Ru, Pt)

and transition metals (Co, Fe, Ni, Cu). Pioneering studies have been focused on Fe-based materials [59], due to their activity in relation to the synthesis reaction, while in the last few years, studies have been more closely focused on noble metal catalysts, with a particular focus on Ru-based materials [60]. These noble metal-based catalysts enhanced ammonia decomposition thanks to the reaction affinity between ruthenium and nitrogen. Ru is the most widely investigated element due to its high turnover frequency (TOF), in the order Ru > Ir > Rh > Ni > Pt > Pd > Fe [58]. Considering the high cost of Ru, several strategies have been proposed to reduce the catalyst cost or improve its activity. The first approach is the modification of the intrinsic activity by changing the catalyst's morphology. Indeed, a decrease in Ru particle size usually increases the number of active sites available for the reaction. On the contrary, it is important to remember that a smaller dimension of the particle leads to higher surface energy, enhancing particle agglomeration in long-term applications [61]. Based on Chen et al.'s analysis [60], a Ru particle size close to 8 nm seems to be optimal for catalytic activity and long-lasting performance.

A further topic of concern in the current research is the reduction in noble metal load. It has been proven that the activity of a catalyst can be enhanced both by the addition of a promoter and the selection of a proper supporting phase. As regards the promoters, it has been previously reported in relation to ammonia synthesis that the presence of small amounts of transition metals, alkali, or alkali or rare earth metals, can improve catalytic activity, and this characteristic remains valid for the ammonia decomposition process [62]. Despite the fact that the role of promoters is still under debate, the results suggest that the presence of such compounds enhances both the kinetic rate and the stability over time. Interesting results have recently been obtained [63]. Sayas et al. [64] decreased the Ru-load by using nanosized particles (7 nm) coupled with K as promoters on the CaO support, and a complete ammonia conversion was reached at lower temperatures (from 550 °C to 480 °C). For the authors, the presence of potassium hindered competitive H_2 adsorption. Promoters also have a beneficial effect on the activity of free-noble metal catalysts, such as Barium in Co–Ce catalysts [63]. The microkinetic modeling proposed by Lezcano identified that the Ba addition enhances the rate of N_2 desorption, which is one of the suggested kinetic-limiting steps.

Regarding the catalyst support, although it is not directly involved in the reaction, it can provide important features, such as an improved dispersion of the catalytic phase, high surface area, non-acidic environment, and good thermal and electrical conductivity. Promising results have been obtained with Al_2O_3, which is widely used in many catalytic processes, as well as with other metal oxides or alloys, such as SiO_2 [65], Y_2O_3 [66], Sm_2O_3 [67], CeO_2 [68], and $La_{0.8}Sr_{0.2}AlO_3$ [69]. Possible alternatives for support, which are currently under investigation, include carbon materials due to their high tunability in terms of both shaping and chemical properties [70,71]. Recent studies have focused on doping carbon with heteroatoms (nitrogen, oxygen, and sulfur) and CNTs [72,73]. If the decomposition is affected by the electron transfer rate, then a highly conducting support can improve process performance. In this regard, the presence of impurities introduces defects that have a beneficial effect on electric conductivity.

2.2. Methanol

2.2.1. Methanol Production

The interest in methanol as a hydrogen carrier has increased due to its relatively high content of hydrogen (12.5 wt. %), low volatility at ambient conditions (T_{eb} = 64.7 °C), and compatibility with the existing infrastructure for storage and transportation. Considering the impact of this topic on scientific research, a separate section is dedicated to this LOHC; Section 2.3 concerns formic acid, while Section 2.4 will be dedicated to describing more complex organic compounds that have been considered in the last few years. In 2023, Lee et al. [19] referred to the view of George Olah regarding the development of the methanol economy [74]. The employment of carbon-based hydrogen carriers, such as methanol, fits the requirements for energy transition and achieving net-zero carbon

emissions. Here, sustainable methanol production must be the result of the integration of carbon capture and storage (CCS) technologies and green hydrogen generation [75].

The interest in methanol is also confirmed by the annual production, which has been undergoing a rising trend. In 2022, the global production has been estimated at 100 Mt and the forecast is for an increase up to 190 Mt in 2030 [76]. Different approaches have been made available at the industrial scale, as a function of composition feed. Natural gas, coal, and biomass have been widely used as carbon sources for this synthesis. Nevertheless, it has been reported that the aim of this review is the evaluation of CH_3OH as hydrogen carriers, and its production acquires environmental relevance if the reaction pathway is based on sequestrated CO_2 and green H_2. For this process, the most diffuse approach is based on heterogeneous catalysis with copper/zinc oxide (Cu/ZnO) [77]. The most active and stable catalytic systems are $CuO/Zn/Al_2O_3$ and $Cu/Zn/Al_2O_3$. This hydrogenation process is characterized by quite low conversion rates [78], and it occurs in temperature and pressure ranges of 220–350 °C and 20–100 bar, respectively. Indeed, some studies show that if pure CO_2 is used as a carbon source the process is less effective than when CO is contained in the feed. An early study [79] showed that at 70.92 bar and 250 °C, the process with pure CO_2 had a yield of 50%, which increased up to 72% with a mixture of CO/CO_2 (x_{CO} = 0.4). In 2018, Marlin et al. [80] evaluated the impact of synthesizing CH_3OH with CO_2 rather than CO. Carbon dioxide is less reactive than carbon monoxide, and for this reason, larger reactors are required. The advantages of operating with CO_2 are its higher selectivity towards the desired product, milder reaction conditions, and a less complicated and lower-cost vessel design.

When looking for a more sustainable methanol synthesis method able to operate at milder conditions, CO_2 electrochemical reduction seems to be one of the most promising routes [81,82]. Process performances are affected not only by the selection of the electrocatalysts, but also by the operating conditions and reactor design. Most of the efforts have been focused on the synthesis of electrode materials selective towards methanol formation, which involves the transfer of six electrons and suffers from the competition related to faster hydrogen evolution. Further to the traditional issues that can affect the electrochemical conversion process (low selectivity, mass transfer limitations, high overpotentials), a further important aspect to consider is the low CO_2 solubility (1.69 g/L at 20 °C and ambient pressure).

The electrochemical generation of methanol occurs at the cathode where the CO_2 reduction takes place. As reported in Figure 3, there are several competitive and more favored reactions that can decrease the overall efficiency; as such, it is necessary to identify suitable conditions (electrode material, solution composition, pH, temperature, pressure, CO_2 concentration) to promote CH_3OH production.

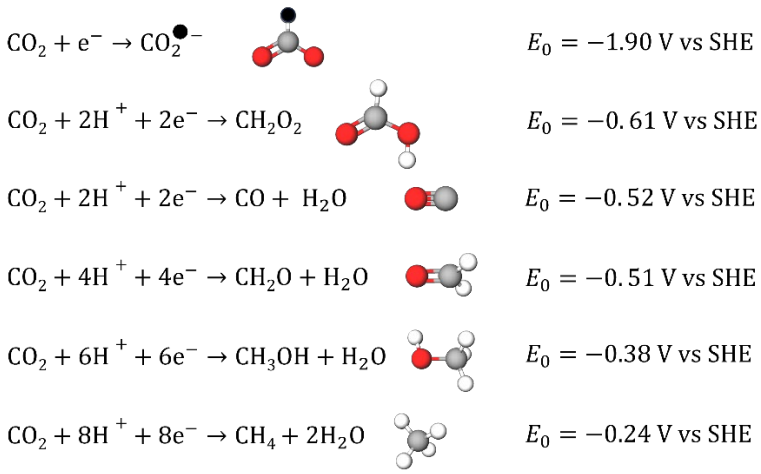

Figure 3. Possible reactions at cathode surface during electrochemical CO_2 reduction for methanol synthesis. Figure adapted from [81].

Independent of the final product, the initial step in the formation of the $CO_2^{\bullet-}$ radical affects the process with a high overpotential (−1.90 V vs. SHE). This feature, coupled with the aforementioned low CO_2 solubility, requires targeted actions on the electrode material and the solution composition (e.g., organic solvents to increase CO_2 solubility), and a proper reactor design for enhancing mass transport [36]. The design of a suitable cathode for commercial application must consider high methanol selectivity, high Faradaic Efficiency (FE), and long stability under operating conditions. The application of pure metals is not suggested due to their low efficiency, and more complex compositions are preferred, such as metal oxides and alloys. The selection of metal oxides (MO: Cu_2O, RuO_2, TiO_2, MoO_2, Co_3O_4) as the electrode material is justified by their basic behavior that improves CO_2 adsorption on cathode sites [81]. One of the limitations related to MO is the lack of high electrical conductivity, which can negatively affect the charge–transfer resistance. In resolving this issue, approaches such as nanostructured morphology and couplings between different materials have been proposed. Weak Cu_2O cathode performances have been improved by Albo et al. [83] by mixing them with ZnO. The authors considered different Cu_2O/ZnO weight ratios, and the maximum methanol formation rate was reached with a ratio of 1:1 at −1.3 V vs. Ag/AgCl (3.17×10^{-9} mol cm^{-2} s^{-1}, FE = 17.7%). In 2021, Guo et al. [84] reported a strong improvement in FE (FE = 88.6%) when using a MO-based system by dispersing an atomic Sn site anchored on a defective CuO catalyst. In this case, the enhancement is derived from the cooperation between Sn site–oxygen vacancy–CuO, with the formation of a double-layer capacitance, larger CO_2 adsorption capacity, and lower charge–transfer resistance.

Recently, some promising results have been obtained using metal alloys. Huang et al. [85] coupled the Sn–Zn bimetallic system with a 4-aminopyridine (Py) organic catalyst supported on carbon paper. A FE = 59.9% for methanol was reached and kept stable for more than 25 h due to the synergic effect between the bimetallic system and the organic compound. An impressively low potential for selective methanol production has been determined by Bagchi et al. [86] with a $CuGa_2$ catalyst. Electrochemical CH_3OH synthesis occurs at −0.3 V vs. RHE and with a FE of 77.26%, optimizing cell design with a flow–cell reactor.

2.2.2. Hydrogen Release from Methanol

The release of hydrogen from methanol requires a mild temperature (200–300 °C) due to the absence of C–C bonds, and the most diffuse path is the catalytic steam reforming of methanol (SRM). In this process, it is extremely important to ensure the correct selection of operating conditions and catalysts to minimize CO production, which is both highly toxic and can introduce poisoning issues in downstream applications (e.g., PEMFC) [81,87]. For these reasons, in methanol-to-hydrogen conversion, the cracking reaction is often coupled with water gas shift, as reported in this reaction pathway:

$$CH_3OH + H_2O \rightarrow CO_2 + 3H_2 \qquad \Delta H^\circ_{298K} = +49.7 \text{ kJ mol}^{-1} \quad (2)$$

$$CH_3OH \rightarrow CO + H_2O \qquad \Delta H^\circ_{298K} = +90.7 \text{ kJ mol}^{-1} \quad (3)$$

$$CO + H_2O \rightarrow CO_2 + H_2 \qquad \Delta H^\circ_{298K} = -41.2 \text{ kJ mol}^{-1} \quad (4)$$

The commercial catalyst composed of Cu/ZnO/Al_2O_3 shows high activity towards hydrogen and low selectivity for CO, due to a synergistic effect between Cu and ZnO. Nevertheless, its stability over time is still an open issue due to the segregation of ZnO, particle agglomeration, and the deposition of carbonaceous compounds leading to a progressive loss of active sites. Different strategies have been applied to overcome these issues [88]. Cheng et al. [89] added magnesium to a CuZnAl–xMg formulation, identifying the optimum level for catalytic activity at 5% = Mg. The addition of Mg promoted the substitution of Cu^{2+} in the malachite phase of the catalyst precursor with Cu^+, while the stability allows for improved interactions between Cu and ZnO.

A second group of catalysts for SRM is based on nickel, which is less active than Cu and other noble metals, and it usually works at higher temperatures (250–500 °C). On the contrary, Ni provides good mechanical strength and higher resistance to poisoning. Ni shows non-negligible interactions with carbon, meaning the deposition of methanol coke with the formation of NiC is possible [90]. The presence of oxygen atoms could improve the selectivity of Ni, thus reducing carbon deposition. In this regard, in 2022, Shen's group [91] proposed a Ni-based catalyst, focusing on its recyclability. They prepared a series of NiO/NaF systems, wherein the oxide is the active phase and NaF is the supporting phase. Catalysts with different loadings of NiO have been considered, and the 6% NiO/NaF showed the best performance, with 94% CH_3OH conversion, 100% H_2 selectivity, and 30 h of stable operation at 450 °C. The recyclability of catalysts has been successfully tested, and after water washing followed by acid washing, the activity was restored to the initial values.

The catalyst's stability can be enhanced using noble metal catalysts, which also have high stability at high temperatures. Improved stability has been achieved by substituting the copper with palladium, such as in PdZn catalysts, but this introduces a twofold drawback. Pd is a PGM with impacts on costs, and it is less active than Cu in the desired reactions. A promising approach seems to the coupling between these two elements (Pd, Cu), and their alloys showed both high catalytic activity and longer stability [92].

2.3. Formic Acid

2.3.1. Formic Acid Production

Several studies focused on using formic acid (CH_2O_2, FA) as a possible hydrogen carrier, despite its gravimetric H_2 capacity (4.4 wt. %) being lower than the desired 5% [37,93,94]. This interest is also justified by the well-established knowledge regarding its handling, as well as its low toxicity, and the mild conditions required by the dehydrogenation process [95,96]. From an industrial point of view, formic acid is mainly produced via the hydrolysis of methyl formate derived from methanol carbonylation. A second route of FA synthesis is as a coproduct in acetic acid production [97]. Nevertheless, the usage of formic acid as a hydrogen carrier gains appeal if the synthesis route is based on captured CO_2, as proposed for methanol synthesis. The reaction can ensue via heterogeneous thermocatalysis, as well as with homogeneous catalysis or in innovative electrochemical systems. As regards heterogeneous catalysis for the conversion of CO_2 to FA, it is favored at high temperatures and high pressure. Due to these harsh conditions and the difficulties in formic acid selectivity, few works have focused on this reaction pathway [98]. The first catalyst for heterogeneous formic acid synthesis was proposed in 1935, and it was based on RANAY® nickel, operating between 200 and 400 bar and 80 and 150 °C. Some improvements have been reached by employing noble metal catalysts such as Pd/C, but due to the interaction of formate with carbonaceous support, low conversion has been observed [35]. These weaknesses shift the efforts towards homogeneous catalytic systems. In homogeneous catalysis, Ru-, Rh-, Ir-, Pd-, Ni-, Fe-, Ti-, or Mo-based material have been proposed for the hydrogenation of carbon dioxide in CO_2, both in water or in other kinds of solvents such as dimethyl sulfoxide (DMSO) [37]. The activity is sensitive to the pH of the solution wherein the reaction takes place. Enhanced activity has been identified in a system containing a base because the subtraction of protons forces the desired reaction [98]. When the reaction occurs in water, polar solvents or basic compounds such as sodium hydroxide or carbonates are usually used, while amines are preferred as organic media. Another parameter to consider is that the solubility of CO_2 in solution is quite low, and a large-scale process could require an extremely high volume. For overcoming this limitation, some works have proposed operating under supercritical conditions. In the work of Puring et al. [99], supercritical CO_2 was coupled with the electrochemical reduction of carbon dioxide for a more sustainable process, as already discussed for methanol [100]. In this study, the cathode is made up of copper on a carbon-based support, and the supercritical CO_2 conditions, with a pressure of 150 atm, drastically reduced the hydrogen evolution reaction and enhanced the current efficiency, yielding a higher level of formic acid production (Figure 4).

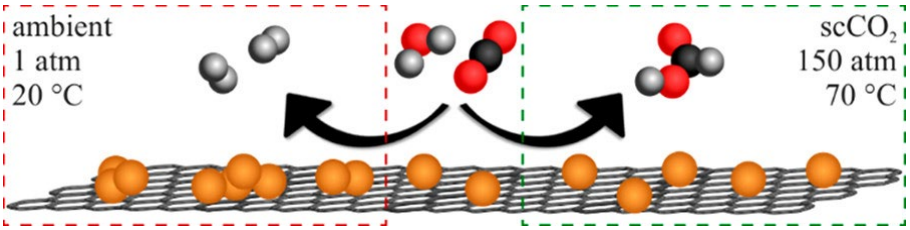

Figure 4. Schematic comparison of CO_2 reduction for formic acid synthesis at ambient conditions (left side) and supercritical CO_2 conditions (right side). From [100].

2.3.2. Hydrogen Release from Formic Acid

In the dehydrogenation reaction of FA, the first target in selecting the operating conditions and the catalyst is the inhibition of the reaction (6) with CO formation, due to safety issues and the deactivation of the catalyst:

$$CH_2O_2 \rightarrow CO_2 + H_2 \quad (5)$$

$$CH_2O_2 \rightarrow CO + H_2O \quad (6)$$

Homogeneous catalysis has also been widely studied for hydrogen release from FA [101,102]. The most widely used catalytic systems are based on soluble metal complexes selective towards the reaction (5). PGM-based catalysts (Rh, Ru, Ir) and Fe-based compounds have been investigated. The first works proposed phosphine complexes such as $IrH_2Cl(PPh_3)_3$ and $Rh(C_6H_4PPh_2)(PPh_3)_2$. The Ir-based complexes show the best decomposition kinetics with a rate of 7.36 mol l^{-1} h^{-1}. Noteworthy results were obtained in the early 2000s by Laurenczy and Beller [103] with Ru–phosphine catalytic systems, which allowed for selective FA dehydrogenation without the formation of CO. In the last few years, research activities have been focused on the development of water-soluble catalysts active in the absence of organic additives for higher environmental sustainability [102]. In greater detail, the results available in the literature suggest that the catalytic activity of metal is highly affected by the electro-donating ability of the ligands to the metal. This hypothesis has been confirmed by Onishi et al. [37,102], who considered Cp*Ir complexes (where Cp = pentamthylcyclopentadienyl) bearing 2,2′-bipyridine. The catalyst with the unsubstituted ligand had a low activity (TOF = 30 h^{-1}), while the introduction of electro-donative OH groups at 4,4′-position of bipyridine massively improved the performance (TOF = 2400 h^{-1}). A further improvement can enable operation in a closed reactor, due to the spontaneous increase in the pressure during the reaction.

The current research is also dedicated to the development of heterogeneous catalytic systems. Interest in this area has increased due to the easier separation of two different phases and the higher recyclability of such materials, which also attracts industrial stakeholders. Metal nanoparticles are attracting the attention of several groups [104–106], because of their high catalytic activity. Some aspects must be considered in the preparation of metal nanoparticles, such as the agglomeration of small particles during the sintering stage due to their high surface energy, and the interaction between the metal-dispersed phase and the support. Hydrogen release from formic acid has been obtained using Au, Pd, Ir, Pt, and Pd on carbon and alumina. For example, nanosized gold particles finely dispersed on an Al_2O_3 support provided high activity and low CO production [37].

2.4. Liquid Organic Hydrogen Carriers (LOHC)

2.4.1. Introduction to LOHC Loop

The usage of liquid organic compounds as hydrogen carriers requires unsaturated molecules that can host hydrogen [107]. Indeed, the LOHC-based systems work by coupling an unsaturated compound with its saturated form by means of a hydrogenation–dehydrogenation loop, as reported in Figure 5. The interest in LOHC is justified by the possibility of storing hydrogen at room temperature or milder conditions than CH_2 and

LH_2 methods, and by the reduced production of CO_2 and N_2, as happens when CH_3OH and NH_3 are used, respectively. Moreover, in some cases, the chemical nature of LOHC means that their storage and transport can rely on the exploitation of infrastructure already available in the petrochemical sector, such as tanks and pipelines, with a positive impact on investments.

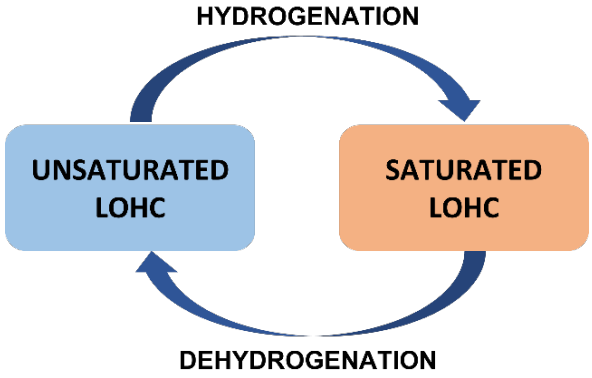

Figure 5. Loop for liquid organic hydrogen carrier.

Hydrogenation is a catalytic reaction that occurs at high pressure (10–80 bar) and intermediate temperature (100–400 °C) with heat release, which can be exploited in the energy balance of the system [36]. The industrial interest is focused on LOHC, which can provide a hydrogen capacity of at least 5 wt. % [78]. Other distinguishing factors that drive LOHC selection are the synthesis process (easy and cheap), the toxicity of the compounds and the risk associated with their handling, and the complexity of final hydrogen release. The dehydrogenation process is an endothermic reaction, requiring an energy supply, and it is usually set as the limiting stage; its sustainability is evaluated by considering two key parameters, such as the temperature required by the process and the enthalpy associated with the reaction. Then, the development of an LOHC-based system relies on the energy balance of the whole process, as well as the recycling efficiency of organic molecules and catalysts.

Several classes of organic compounds have been considered as LOHC, and among them, aromatic compounds have been identified as the best option, as was recently confirmed by Chu et al. [108]. As previously introduced, a complete study on LOHC must take into account both the key steps (hydrogenation, storage, transport, and dehydrogenation). This review discusses the most promising organic couples that have been reported in the literature in the last few years.

2.4.2. Benzene–Cyclohexane Loop

The most investigated system is benzene (BNZ)–cyclohexane (CHX), due to its high hydrogen capacity (7.2 wt. %). The saturation of BNZ to CHX occurs at 150 °C and 40 bar, and homogeneous catalysis has been considered for hydrogenation, but the results show a lower efficiency and stability compared to the heterogeneous catalytic systems [37]. Bianchini et al. reported that the complex $[Rh(5\text{-}C_5Me_5)Cl_2]_2$ is active in the hydrogenation of benzene to cyclohexane at 50 °C and 50 bar, and with a base acting as a promoter [109].

The bottleneck of the BNZ–CHX loop is the temperature required for hydrogen release (~300 °C), as is typical for an LOHC-based process, as well as the catalytic selectivity with the possible formation of several by-products (e.g., cyclohexene, cyclohexadiene) and the resulting decrease in process recyclability. As expected, Pt was one of the first materials to be considered as a catalyst, but the latest studies are focused on more active and selective materials. Nevertheless, some materials recently proposed still contain Pt mixed with other elements. Wang et al. [110] recently studied the catalytic performance of PtPd alloy nanoparticles supported on nitrogen-doped carbon. The experimental results show the excellent catalytic activity with a TOF of 90.07 mmol g^{-1}_{metal} min^{-1} and 100% H_2 purity

at 180 °C. The density functional theory (DFT) calculations suggest that the presence of Pd promotes the specific adsorption and activation of CHX on the Pt surface. A similar enhancement has also been seen when substituting Pd with Ru and Ir [110]. Extraordinary Pt activity enhancement in a reversible hydrogenation–dehydrogenation catalyst has been described by Chen et al. [111]. Here, single Pt atoms were supported on CeO_2 nanorods, and this system allowed a performance increase of 309 times compared to conventionally supported nanoparticles. Noble-metal-free catalysts based on Fe, Ni, Cu, and Zn have been considered. Many efforts have been directed towards Ni-based materials. The main issues with Ni are the high hydrogenolysis, which leads to a low selectivity for cyclohexane to toluene. In this category of catalysts, a widely used strategy consists of the addition of a second transition metal. Despite the results remaining very different from those reported for noble-based catalysts, the Ni–Cu bimetal system supported on activated carbon cloth (ACC) showed a performance improvement [112]. The NiCu/ACC has a CHX conversion and H_2 yield of 25.78% and 19.41%, respectively, versus a CHX conversion of 7.64% and a H_2 yield of 5.75% for the Ni/ACC material. The positive effect of copper on nickel activity was confirmed by Xia et al. [113], using a $NiCu/SiO_2$ system. In this case, the addition of copper and the presence of SiO_2 as a supported phase provided excellent selectivity for hydrogen release and benzene (99.5%) at 350 °C.

2.4.3. Toluene–Methylcyclohexane Loop

The couple toluene (TOL)–methylcyclohexane (MCH) has been widely considered due to its hydrogen capacity (6.2 wt. %), the mild toxicity of the MCH, and the low cost of chemicals [114]. Moreover, both TOL and MCH are liquids under ambient conditions. As regards the hydrogenation process, conventional catalysts based on Pt are used, with a non-negligible impact on cost. In the last few years, low-Pt-content and Pt-free catalysts have been proposed in the search for high catalytic activity and poisoning resistance. Indeed, when Pt is used, an ultrapure H_2 feed (>99.99%) is required to avoid its deactivation [115]. Many catalytic-supported systems have been proposed [116]. Alumina (Al_2O_3) is usually the supporting phase, functionalized with a transition metal such as Ni, Co, or Mo. Nevertheless, these catalysts provide lower activity than Pt towards hydrogenation, requiring more severe operating conditions. Zhou et al. [116] proposed an Fe-promoted Mo carbide catalyst; they investigated the effect of iron load (Fe:Mo ratio) and carburization temperature (550–700 °C) on catalytic activity and stability. The addition of iron slightly affects the hydrogenation activity, while strongly improving the stability over time. The observed degradation has been attributed to surface oxidation, and a re-carburization treatment can recover the initial properties of the catalysts.

Recently, Wang et al. [115] addressed CO catalysts' deactivation, proposing an innovative Pt-free catalyst made of $RuNi/TiO_2$, which also promotes toluene hydrogenation in the presence of carbon monoxide in a range of 1000–5000 ppm. A further positive effect is represented by the mild operating conditions (atmospheric pressure and 180 °C) required. The improvement is related to the different bonding properties of Ru and Ni, which interact with CO and toluene, respectively.

Nagasawa et al. [117] reported the promising electrohydrogenation of TOL using a solid polymer electrolyte setup. The main advantage of such a process is the coupling of hydrogen production by water electrolysis with toluene reduction in one reactor, according to the following reaction scheme:

$$\text{Anode: } 3\,H_2O \rightarrow 3/2\,O_2 + 6H^+ \qquad E^\circ = 1.23\ \text{V vs. SHE} \tag{7}$$

$$\text{Cathode: } C_7H_8 + 6H^+ + 6e^- \rightarrow C_7H_{14} \qquad E^\circ = 0.154\ \text{V vs. SHE} \tag{8}$$

In this system, of concern is the development of an electrocatalyst able to favor the hydrogenation of TOL to MCH, rather than hydrogen evolution, which is a competitive reaction. The results show that a cathode made of carbon paper loaded with Pt is able to sustain the desired reaction, highlighting the importance of the cathode layer's thickness

and the catalyst load, as well as the high impact of mass transport features typical of the electrochemical systems. Electrochemical hydrogenation has also been investigated by Imada et al. [118], using a binary Pt-based alloy nanoparticle-loaded (50 wt. %) carbon catalyst (Pt_3M/C). The authors considered several binary systems (Pt_3M) with different metals (M = Rh, Au, Pd, Ir, Cu, and Ni), and the presence of metal boosts the activity of commercial Pt/C. PtRh/C provides the highest activity, and the Tafel slopes obtained for each catalytic system suggest that the kinetic mechanism is not affected by the metal.

The MCH dehydrogenation process is mainly based on Pt catalysts with a non-negligible impact on process costs, which are also affected by the energy input required by the endothermic reactions. Therefore, the main efforts made have been towards reducing the amount of Pt in the catalytic formulation and decreasing the operating temperature. Nevertheless, the replacement of Pt-based catalysts is not trivial due to the high catalytic properties with a toluene yield of up to 99% [119]. Bimetallic catalysts seem to be a promising alternative, as reported by recent studies [37]. Increasing interest has been shown in catalytic systems containing Ni coupled with a second transition metal. The presence of such elements (Cu, Zn) reduces the activity of Ni towards the hydrogenolysis of the C–C bond, increasing the selectivity towards toluene up to 97%.

An alternative strategy to reduce cost has been proposed in [120]. Lv et al. developed a nickel single-atom cerium oxide catalyst to be used in a solar-heating catalytic MCH dehydrogenation reaction. The H_2 generation reached a rate of 2756 mmol g^{-1} h^{-1} at 400 °C, and the design of the thermal catalytic device allowed for operating under solar irradiation, without a secondary energy input.

A factor that can be considered during the dehydrogenation step is the recovery of heat. Pashchenko [121] described the thermochemical recuperation of waste heat during hydrogen extraction from LOHC, considering as a model the MCH–TOL system. The thermodynamic analysis performed in temperature and pressure ranges of 100–400 °C and 1–4 bar, respectively, showed maximum thermal efficiencies at 300–350 °C and 1.5–2 bar. These conditions allow for obtaining an acceptable MCH conversion rate and notable separation between hydrogen and toluene.

2.4.4. Naphthalene–Decalin Loop

The naphthalene (NPT)/decalin (DCL) system is characterized by a hydrogen capacity of 7.3 wt. %, and it has been considered as a possible hydrogen carrier in the last few years [122]. Conventional catalytic systems for NPT hydrogenation operate in temperature and pressure ranges of 250–400 °C and 15–80 bar, respectively. A recent thermodynamic and kinetic analysis carried out by Peng et al. [123] suggested that the optimal conditions for NPT hydrogenation when using a commercial NiMo/HY catalyst are 400 °C, 80 bar, and a ratio of H_2/NPT equal to 4. The addition of hydrogen to NPT molecules can lead to the formation of several by-products and aromatic hydrocarbons (e.g., tetralin, butylbenzene, ethylbenzene), and to avoid this, it is necessary to seek an improvement in catalyst selectivity towards decalin. Promising results have been obtained by Ma et al. [124] by means of a surface-engineering approach. The molybdenum carbide (α-MoC) surface was doped with Pd, and the addition of the noble metal promoted the generation of vacancies in the Mo structure, as well as the selective hydrogenation of NPT to DCL. The authors also investigated the dopant load, finding that the optimum performance corresponded to 0.5 wt. % of Pd.

The saturation of naphthalene to decalin is favored when metal nanoparticles are used as catalysts [125]. In the last few years, studies have also been dedicated to non-noble metal catalysts. For these materials, possible actions to improve their activity relate to the selection of the support and the synthesis method, or metal loading. Vargas et al. [126] prepared Ni catalysts (4 wt. %) supported on SBA15 (amorphous silica) and Al-SBA15. The results show that the addition of Al into the SBA15 structure caused the substitution of Si^{4+} with Al^{+3} and the formation of Brönsted acid sites. This change had a positive effect on catalytic activity, which was also influenced by the preparation route. Indeed, a higher activity

was reached when the EDTA was used as a complex agent during catalyst loading on the support, rather than using nickel nitrate. The enhancement in selectivity in the presence of EDTA is related to a better dispersion of the Ni particles and a greater amount of acid sites. Nevertheless, these catalytic formulations are not able to compete with noble metal-based catalysts at present. Therefore, part of the research is focused on how reductions in catalyst load preserve the activity. As previously introduced, the performance of a supported catalytic system depends on the intrinsic activity of the metal phase and its interaction with the supporting phase. Zhang et al. [125] evaluated this relation in a catalytic system made up of Pd supported on HY zeolite (SiO_2/Al_2O_3). A detailed investigation allowed for the determination of the most suitable SiO_2/Al_2O_3 ratio, and the role played by the active metal, acid sites, and zeolite mesopores' volume in catalytic performance.

Most of the studies regard the dehydrogenation stage, which is the limiting reaction of the whole process in LOHCs. Beyond pure noble metals, other catalytic systems have been proposed. The current leading approach to catalyst development is based on a multicomponent system, with the aim being to exploit synergistic effects. In some cases, noble metals are coupled with a suitable support. In 2023, Luo et al. [122] investigated the synergy of Pt and Pd in a bimetallic system. Firstly, the authors identified the optimum Pt load (3 wt. %) when $MgAl_2O_4$ is used as the supporting material. They also investigated a PtPd bimetallic system (Pt:Pd = 4:1) dispersed on the same spinel structure. The synergistic effects of the bimetallic catalysts allow for decreasing the amount of the catalyst by up to 1%, while preserving the performance. The selection of $MgAl_2O_4$ as a supporting phase is justified by the results recently presented by Wang et al. [127]. This material has been compared with other candidates used as supporting phases, such as Al_2O_3, mesoporous silica (MCM-41), and active carbon (AC). The results clearly show the improvement correlated with the usage of $MgAl_2O_4$ due to the higher dispersion of Pt particles, which allows the formation of smaller nanoparticles (average size of 1.24 nm) with enhanced activity. The authors also underlined the strong effect of the method of synthesis of the supporting phase, and how properties such as crystallinity, morphology, and surface acidity can affect the catalytic performance.

2.4.5. Dibenzyltoluene–Perhydrodibenzyltoluene Loop

The dibenzyltoluene (DBT)/perhydrodibenzyltoluene (18H-DBT) system with a hydrogen capacity of 6.2 wt. % has gained attention as an LOHC also due to the well-established industrial production of DBT and its competitive price (EUR 2–4/kg), and the extensive knowledge related to safety and handling issues [35,128]. The dehydrogenated product (DBT) is noncarcinogenic and nonexplosive, representing a fairly rare advantage related to benzene and its derivatives. Moreover, 18H-DBT has the main advantage of being liquid and stable in a wide temperature range (−30 to 360 °C). From a technological point of view, the DBT–18HDBT loop shows excellent reversibility with a remarkable kinetic rate and a competitive dehydrogenation enthalpy (65.4 kJ mol^{-1}). As regards DBT hydrogenation, a relevant reaction rate has been obtained by using a Ru/Al_2O_3 heterogeneous catalyst, which worked better than the Ru/C and Pd/Al_2O_3 catalytic systems [35].

Hydrogen quality can influence the performance of the hydrogenation stage. Jorschick et al. [128] investigated hydrogen storage in 18H-DBT in a temperature range of 150–260 °C, evaluating the effect of wet hydrogen. Firstly, Ru and Rh have been identified as very active for DBT hydrogenation below 200 °C. The presence of water in the hydrogen stream can affect catalytic activity, but at the same time, the authors underline that the amount of water used in that research is several orders of magnitude greater than the real application value. Further, these results suggest that it is possible to identify catalysts that are active with wet hydrogen, avoiding the dry stage between the electrolysis and hydrogenation, with a relevant impact on the overall energy consumption of the process.

The noble metals remain the reference catalysts for dehydrogenation, as reported by Bruckner et al., who considered Pt and Pd on different supports (Al_2O_3, SiO_2, C) at 270 °C [129]. The Ru/Al_2O_3 catalytic system also provided promising activity in mild conditions, operating at 10 bar and in a temperature range of 80–160 °C [129].

Another route to increase the process performance is the reactor design, and this aspect can play a fundamental role in process scale-up at the industrial level. Indeed, most of the studies carried out at the lab scale have been performed in a stirred tank reactor, which is usually affected by inefficient heat transfer and mass transport. Ali et al. [130] proposed an innovative continuous microchannel reactor, which showed greater hydrogen release compared with the stirred tank, which increased from 64.1% to 82.2% at 320 °C after 20 h. Moreover, this option allowed a decrease in the amount of catalyst used.

In all the LOHC systems proposed above, it is extremely important to avoid a non-uniform temperature distribution within the dehydrogenation reactor [36]. Indeed, the formation of colder zones leads to a slowdown of the kinetic rate. On the other hand, the presence of hot spots can cause the decomposition of the dehydrogenated LOHC form, with the risk of breaking C–C bonds and complicating the compounds' recyclability.

2.5. Metal Hydrides

Metal hydrides (MH) are an interesting solution that can operate under milder conditions than LH_2 and CH_2, with a storage pressure no higher than 30 bar, one order of magnitude lower than compressed hydrogen, simplifying the handling procedure. H_2 reacts with metals or alloys in a reversible reaction, allowing its release, and this solution seems to be promising for small–medium applications (up to 30 Nm^3 H_2) [23,131]. H_2 release is one of the main drawbacks of MH-based system, requiring energy supply due to the endothermal conditions. Moreover, the recovery and reuse of the dehydrogenated metal form is still an open issue that must be faced. Indeed, the development of a storage system based on metal hydrides must be based on loop concept, with the possibility of the recovery of the dehydrogenated form, as already shown for LOHCs, and its regeneration to the hydrogenated form.

A suitable metal hydride system should be able to operate the whole loop (H_2 adsorption/desorption) under conditions close to those of the downstream application. The expected hydrogen capacity of 10 wt. % is a threshold value for metal hydrides. Some materials, such as $Mg(BH_4)_2$ and $LiBH_4$, could theoretically provide a hydrogen capacity of 14.9 wt. % and 18.5 wt. %, respectively, satisfying the requirements, but the operating conditions (pressure, temperature) required for both the hydrogenation and dehydrogenation processes, and the corresponding kinetic rates, are far from targets [132].

Sodium borohydride ($NaBH_4$) has attracted attention in the last ten years due to its noteworthy hydrogen capacity (10.8 wt. %), good hydrolysis management, and excellent hydrogen purity. The hydrolysis mechanism is based on the following reaction:

$$NaBH_4 + 2H_2O \rightarrow NaBO_2 + 4H_2 \quad (9)$$

Nevertheless, from a practical point of view, several drawbacks are blocking the application of such a system as a hydrogen carrier, among them being the production of hydrate sodium metaborate ($NaBO_2 \cdot xH_2O$), which is hard to recycle [133]. Consequently, efforts are being made to develop approaches that will allow a higher selectivity towards H_2 or an improvement in the $NaBO_2$ regeneration process.

Barbucci et al. [134,135] demonstrated that effective thermochemical $NaBH_4$ regeneration can be obtained when working over 600 °C and 12 bar. The complete conversion of $NaBO_2$ has been achieved in 90 min at 634 °C and 30 bar of H_2. More recently, Ouyang et al. [133] obtained enhanced regeneration under room conditions by milling sodium metaborate ($NaBO_2 \cdot 2H_2O$ and $NaBO_2 \cdot 4H_2O$) with Mg (molar ratio $NaBO_2 \cdot 2H_2O$:Mg = 1:5, and $NaBO_2 \cdot 4H_2O$:Mg = 1:9). This approach improves both the regeneration yields, with a maximum of 68.55% for $NaBO_2 \cdot 2H_2O$, and drastically reduces of the cost of the reducing method, which requires the dehydration of $NaBO_2$ and the preparation of MgH_2.

The magnesium hydride itself has been attracting the attention of several researchers, and nowadays is one of the most widely investigated metal hydrides for hydrogen storage [136,137]. This is due to its lighter weight compared to more complex metal hydride systems, its hydrogen capacity (7.6 wt. %), its ease of supply, and its accessible costs (in

2023 Mg ~ USD 3/kg). The current drawback that blocks its application at a large scale is represented by the conditions required for MgH_2 synthesis (hours at 400 °C and 30 bar) and the slow kinetic rate of hydrogen release [138,139]. The reaction occurs in a heterogeneous system where the H_2 gas phase interacts with the Mg solid phase. Based on updated knowledge, the rate-determining step is the dissociation of H_2 molecules on the Mg surface, due to electronic configuration. Indeed, this stage is favored in transition metals that have an orbital d that can easily interact with the hydrogen orbital, which is not available for Mg.

Mg dehydrogenation can be enhanced by the addition of catalysts, as was recently reported [140]. In this paper, Kumar Sing et al. proposed a systematic investigation of the effects of catalysts based on transition metals from groups 4–6 (TiO_2, ZrO_2, HfO_2, V_2O_5, Ta_2O_5, CrO_3, MoO_3, WO_3). The results clearly show that the ball-milling dispersion of oxide on MgH_2 enhanced the desorption rate, and the best performances have been achieved using TiO_2, ZrO_2, V_2O_5, and CrO_3, with promising performance results around 200 °C. The analysis suggests that the process benefits transition metals with multi-oxide states 2^+ and 3^+. Dong et al. [137] used ab initio molecular dynamics simulations to describe the positive effects related to the formation of a heterojunction between MgH_2 and the single-atom catalyst (MgH_2/SAC) by using transition metals. Although the calculations identified a reduction in the activation energy for hydrogen desorption, the authors underline the need for further investigations to achieve a deeper comprehension of the mechanism, and the better tailoring of the material properties. Ismail [24] proposed to destabilize MgH_2 stability with the addition of $NaAlH_4$. The resulting Mg–Na–Al system has a lower decomposition temperature, superior cyclability, and improved kinetic performances, due to the formation of $Al_{12}Mg_{17}$ and $NaMgH_3$ in situ during H_2 release.

A valuable approach for improving the performance of metal hydrides that requires further investigation is nanostructural engineering [132]. The reduction in particle size has a positive effect on the surface thermodynamic properties, as was predicted in 2005 by Wagemans et al. [141]. More recently, the effects of particle size on Mg-based metal hydrides have been reported, with a performance enhancement achieved by decreasing the particle size to lower than 10 nm. Future studies, seeking a full comprehension of the mechanisms that act on the nanostructured systems, must be devoted to evaluating their stability over time, due to the possible agglomeration issue related to the high-energy surface. An example of the effectiveness of reducing particle size has been reported by Zhang et al. [142]. They successfully produced ultrafine MgH_2 nanoparticles (4–5 nm) with a hydrogen capacity of 6.7 wt. % at 30 °C, and furthermore, the first trial of its stability has reported it preserving its performance over 50 cycles at 150 °C.

The discussion presented above for each hydrogen carrier highlights the current challenges that must be faced, and they are summarized in Table 2.

2.6. Integration with the Downstream Power Processes

All the approaches presented above have a final common stage of hydrogen release. This review is mainly dedicated to hydrogen storage; nevertheless, in this section, the main parameters that must be considered are briefly summarized to give key aspects related to the integration of the storage system and final user. Based on a model wherein hydrogen is fed to a fuel cell for power generation, the key aspects that must be taken into account in full process design are as follows.

- Fuel cell selection

The fuel cell technology changes as a function of the application features (power size, mobile/stationary, continuous/discontinuous), and this affects the requirements of the hydrogen inlet stream. Indeed, the H_2 purity, H_2 mass flow, and operating temperature are strictly related to the selected fuel cell and the application size. Low-temperature fuel cells (e.g., PEMFC), which mainly use Pt-based electrocatalysts, are highly sensitive to hydrogen impurities, such as carbon-based compounds and ammonia. Further, in the case of hydrogen storage, when NH_3 or LOHC is used, a high-purification stage will be necessary, affecting the plant cost. On the contrary, high-temperature fuel cells (e.g., SOFC)

are less sensitive to these compounds, and can work easily in the presence of impurities. As expected, the fuel cell operating temperature and pressure will also affect the overall energetic balance, and so it is important to evaluate the matching between the conditions of H_2 release and the fuel cell.

- Storage of CO_2 and unsaturated LOHCs

When hydrogen is stored in a carbon-based compound, we must consider the recovery of the unsaturated LOHCs, as well as CO_2 and CO, when methanol and formic acid are used. This action could impact the process via the challenges imposed on mobile applications, with stricter constraints on the volume and weight of the system.

3. Techno-Economic Analysis

The worldwide use of hydrogen as an energy vector in power applications, and the consequential development of a hydrogen-based economy, require techno-economic analyses for each of the solutions proposed above. The assessment must consider all the stages previously discussions, and the final application (mobile/stationary, continuous/discontinuous) has a strong impact on the selection of the proper technology. Moreover, this section highlights the strong correlation between all the technological factors and the strong influence of policy in developing a hydrogen network. Figure 6 sketches the main parameters that must be considered in a techno-economic analysis. This section addresses the most updates studies on techno-economic analyses of the hydrogen carriers previously introduced.

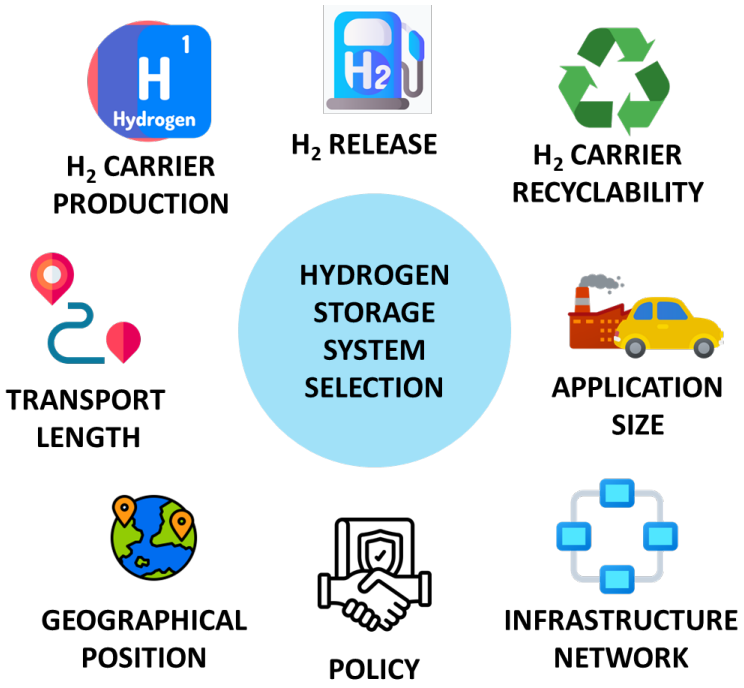

Figure 6. Main factors that must be considered in a techno-economic analysis aiming at the selection of a hydrogen storage system.

In Table 3, the key features that can affect the techno-economic analysis and the selection of hydrogen carriers are summarized and grouped according to the factors introduced in Figure 6. A deeper discussion of these points is given after the table.

Table 3. Summary of the key features of factors that must be considered during the techno-economic analysis of hydrogen carriers.

Factor	Key Features for Techno-Economic Analysis
Hydrogen carrier production	• Hydrogen carriers' production must be coupled with RES to be economically sustainable [143]. • In an RES-based scenario, ammonia-based systems have lower carbon emissions than LOHC, and the minimum cost is reached with the TOL–MCH supply chain [143]. • For RES-based power-to-X solutions (X = hydrogen, methanol, ammonia, and methane), the highest energy efficiency is reached for hydrogen, and the lowest for methane [144]. • The replacement of the Haber–Bosch approach for ammonia synthesis is hindered by the high cost of alternative methods [76]. • The final cost of hydrogen carriers is sensitive to the price of the water electrolyzers required to produce green hydrogen, and to electricity costs [76].
Hydrogen release	• Dehydrogenation of LOHC has too high a cost for large-scale applications [145–147]. • For industrial applications, the integration of the endothermic hydrogen release stage with industrial waste heat can improve economic sustainability [145].
Hydrogen carrier recyclability	• For carbon-based hydrogen carriers, it is necessary to evaluate the economic impact of CO_2 capture technologies (for methanol and formic acid) and the recovery of unsaturated LOHC after hydrogen release [148–150].
Application sector and size	• The shipping industry is one of the hardest sectors to abate due to severe constraints regarding weight and volume, coupled with high power demand [151]. • In the shipping sector, the key parameters to be considered for evaluating techno-economic sustainability are the ship's size and the navigation time [151]. • PEMFC fed by H_2 has been shown to be the most economic option for trips up to 7 days, while on-board CH_3OH steam reforming can be considered for a longer time, and ammonia only if an SOFC is used [151]. • For sizes larger than 5 MW, new technologies stop being able to substitute internal combustion engines in the shipping sector [152]. • Regarding the substitution of diesel-powered trains with hydrogen carriers, metal hydrides are not suitable due to process layout, as well as LOHC. Possible solutions could include using ammonia and CH_2 [153].
Infrastructure network	• Importance of the availability of a renewable energy sources grid [154]. • The choice of the hydrogen carrier has a strong impact on the development of correlated infrastructure, such as port refueling stations [155].
Transport Length	• Transport has a strong impact on small–medium H_2 production [154]. • For small–medium production and long transport distances, the best solution is LOHC [143,154], and CH_2 is best for short transport distances [154]. • Hydrogen exportation as ammonia is competitive if it is directly used; otherwise, LH_2 could be preferred [156].
Geographical position	• The location of the production of hydrogen carriers has a strong impact on process cost [154]. • The decentralized production of hydrogen carriers can represent a possibility for growth at isolated sites [157].
Policy	• Application of incentives [76]. • Increase in carbon taxes [76]. • Necessity to develop a transnational logistic for hydrogen carriers' supply chain [155].

All the factors introduced in Figure 6 and Table 2 are strongly interconnected, and Ibagon et al. [154] discussed the strong interdependency of different factors, such as the availability of RES, production capacity, the kind of electrolyzer, the storage system, and carrier transport. The authors addressed case studies for four different locations in Uruguay.

This example is relevant because Uruguay has a deep renewable energy grid, and this is one of the factors required to have sustainable hydrogen production. It is noteworthy that Ibagon et al. also considered penalties associated with hydrogen production deficits in their simulations. They verified that renewable energy availability is the main factor for large hydrogen demand (250 t_{H2}/d), with a range of 47–57% of the levelized cost of hydrogen (LCOH). The development of an accurate model to forecast renewable energy production is then needed for large-scale applications, along with a deep knowledge of the application site. The transport has a greater impact on small–medium hydrogen productions (1.72 t_{H2}/d and 15 t_{H2}/d), and for such sizes, the best transport options are trucks with liquid organic hydrogen carriers for long distances, and compressed hydrogen for shorter distances.

The integration of the hydrogen supply chain with renewable energy sources and green hydrogen production is vital to decrease the overall production costs and CO_2 emissions. Based on these two assumptions, Lee et al. [143] compared different hydrogen carriers (LH_2, NH_3, TOL-MCH, H0-18HDBT, and methanol) via techno-economic and environmental investigations for large-scale marine transportation. The results show that in a renewable power scenario with green H_2 production, the ammonia system yields the lowest carbon emissions (2.23 $kgCO_2$-eq/kg_{H2}), with an LCOH of 4.92 USD/kg_{H2}, while the lowest cost was achieved with the TOL–MCH supply chain (4.57 USD/kg_{H2}).

The coupling between renewable sources and a power-to-X (P2X) solution has also been discussed by Bellotti et al. [144]. In this work, the authors considered four possible P2X pathways (hydrogen, ammonia, methanol, and methane) produced using RES and a 10 MW PEM electrolyzer. The highest energy efficiency (61.5%) was obtained with power-to-hydrogen (P2H), and the lowest with power-to-methane (45%). Nevertheless, P2H is the worst option in terms of volume required (316 m^3), while the best storage solution in terms of volume and energy density is power-to-methanol (P2M), with a volume of 30 m^3 and 4.3 MWh/m^3. Power-to-ammonia (P2A) is the best solution in terms of H_2 stored in the fuel (108 kg_{H2}/m^3). The economic analysis on expected investment (CAPEX and OPEX) shows that the main costs are related to the electrical energy (50%) and the PEM electrolyzer CAPEX (30%) and OPEX (10%).

The production of hydrogen carriers strongly impacts the economic sustainability of the process. Currently, industrial processes, such as Haber–Bosch for ammonia, are cheaper. Further, it is fundamental to develop strategies of production that reduce the final costs. In 2023, Palone et al. [76] propose a techno-economic analysis of hydrogen generation and storage with a chemical loop derived from waste high-density polyethylene. The work is oriented towards the circular economy approach, and chemical looping, wherein different synthesis processes are coupled, has been used to investigate the simultaneous production of CH_3OH and NH_3. The analysis showed a significant decrease in CO_2 emissions compared with conventional routes. The main operating cost is represented by electricity (66% of overall OPEX), which is also the parameter most prone to fluctuations. On the other hand, the final price evaluation and the competitiveness of such a process are also sensitive to other variables such as the cost of electrolyzers for hydrogen production, as well as the applications of incentives or an increase in carbon taxes.

For the formic acid-based process, the main challenges are the competitiveness of green hydrogen and steam generation for synthesis, which, up to now, are not as significant as the costs of conventional FA production [95]. Moreover, the lack of heterogeneous active catalysts that are easily separable from reaction products hinders the diffusion of the process, which currently bears costs related to the separation and recovery of homogeneous catalysts [158]. In 2016, the techno-economic analysis presented by Pérez-Fortes et al. [148] highlighted the potential of using formic acid as a hydrogen carrier, but at the same time, it underlined the necessity to overcome technological issues related to catalyst development and operating conditions.

The formic acid- and methanol-based processes acquire relevance when coupled with carbon capture and storage (CCS) technologies, and a consequent reduction in overall

emissions can be achieved. Bellotti et al. [150] proposed a techno-economic analysis for the integration of a CCS plant within a coal plant with a system for methanol production. The sustainability of the process is not only dependent on technological design and system integration, but it is heavily influenced by national and transnational policy, and a key role is played by the cost of EU ET CO_2 emission allowances. The integration between carbon-based hydrogen carriers and CCS technologies has also been reported by Cui et al. [149]. In this case, the authors focused on evaluating the cost of transporting hydrogen as methanol and ammonia. Methanol is preferred only at a small scale (<2 t_{H2}/h), and if its synthesis occurs only in the proximity of a CCS plant. Ammonia is more competitive for larger-scale production and in cases wherein an infrastructure for CO_2 capture is not already available.

The literature review highlighted a lower number of techno-economic analyses that consider metal hydrides as hydrogen carrier. Nevertheless, a remarkable techno-economic analysis has been proposed by Rivarolo et al. [159], and the results highlight the advantages offered by metal storage compared with CH_2.

As sketched in Figure 6 and Table 3, the application sector and the required power sizes also influence the selection of hydrogen carriers, and one of the hardest challenges is related to the shipping industry [151]. Up to now, there has been no technology able to completely substitute the currently used fuel engines given the power demand. In the last few years, many candidates have been proposed, such as hydrogen, ammonia, and methanol. As reported by Kistner [151], the navigation time and the ship's size are the most important parameters that must be considered during carrier selection. H_2-fed PEMFCs result as the best economic option for trips up to 7 days. On-board CH_3OH steam reforming could be profitable from both economic and environmental points of view, and for a longer time. Ammonia could be considered only if it is used in the presence of SOFC, but further evaluations of NOx emissions will be necessary.

The complexity of marine sectors and the necessity of differentiating applications has been deeply discussed in [152], wherein a user-friendly tool, called HELM, is presented. The algorithm allows for the direct comparison of different technologies, considering key aspects of the propulsion system such as volume, weight, cost, and emissions, as well as the size of the ship. For small applications (<5 MW), the usage of CH_2 coupled with PEMFC is suggested as an alternative to internal combustion engines (ICEs), while the LH_2 is not so attractive, due to the need for complex auxiliary systems. With an increase in size (>5 MW), the innovative technologies will not be able to completely replace ICE, but the most valuable solutions for use in the future seem to be ammonia and methanol. An on-field marine application has recently been proposed by Cavo et al. [156]. Here, an advanced controlled method has been developed for the thermal management of a metal hydride system coupled with polymer electrolyte fuel cells installed on-board the hydrogen vessel ZEUS. System validation dynamically verified that the heat generated by fuel cells was able to supply the thermal energy required by MH tanks under different navigation conditions and during the transient state. On the contrary, ammonia applications can exploit the advantages of their hydrogen capacity and utilization efficiency, and the low costs of production, along with the possibility to use them directly in NH_3-powered fuel cells.

Another sector currently evaluating the possibility of applying hydrogen power systems is railway transport, in relation to the substitution of diesel-powered trains. The recent analysis of Xu et al. [153] compared different hydrogen carriers (ammonia, LOHC, MH) and the storage of CH_2 and LH_2. Despite its attractive storage density value, the MH application is hindered by the harsh operating conditions that, at the current stage, seem unsuitable for this application. Also, LOHC utilization is not ready to be applied at a large scale due to the harsh conditions required by the dehydrogenation process.

The strong impact of the scale factor has also been discussed in a rigorous economic and environmental analysis performed by Dickson et al. [147], which compared liquid hydrogen (LH_2), ammonia (NH_3), and LNG with methanol, DBT/18H-DBT and TOL/MCH. The scenario of medium-level market penetration favors NH_3 and CH_3OH, with levelized costs of USD 3.6 and 3.78/kg_{H2}, respectively. The LH_2 option becomes competitive at

high-level market penetration, with a cost of USD 2.12/kg_{H2}, due to the strong impact of the dehydrogenation process when an LOHC is used. A positive evaluation of using LH_2 for hydrogen exportation has also been supported by Hinkley et al. [146], who considered a case study of a power station used to produce 600 MW of hydrogen and three different hydrogen carriers. The exportation of H_2 as NH_3 becomes more competitive only if ammonia is directly used, thus avoiding the cracking stage. Nevertheless, NH_3 has the advantage of being easier to ship, along with a well-established knowledge base at the industrial level. The loop TOL/MCH is considered less promising due to the toxicity of the compounds used, and the high energy demand related to H_2 release.

Geographical location affects choices when developing hydrogen-based systems, but at the same time, H_2's economic factors can represent a possibility of growth for isolated sites. Schöne et al. analyzed the potential applications of a decentralized system for hydrogen production in Kenya [157]. The authors pointed out that, despite the promising technological attractiveness of hydrogen-based energy systems, the key to a broad diffusion will be decreasing the costs of such plants.

The interconnection between the factors sketched in Figure 6 is made evident in the case study analyzed by Godinho et al. [155]. Indeed, they not only concluded that LOHC transportation by shipping is sustainable only for short- to medium-distance shipping, but they also clearly showed how the approaches selected for shipping will influence and drive port infrastructure development and related investments, due to the high impact of such a sector on energy demand. In more detail, Godinho et al. highlighted how the economic sustainability of LOHC is strictly related to both technical development and political actions. Favorable transnational legislation in the EU could lead to a logistic cost in the period 2030–2050 ranging between EUR 0.30 and 0.37/kg_{H2} for DBT-PDBT and EUR 0.24 and 0.34/kg_{H2} for TOL-MCH. The promising and competitive prices are also related to the possibility of exploiting existing storage and transportation infrastructures with few modifications.

The sensitivity of H_2 cost to all of the supply chain factors has also been investigated by Zhang et al. [160] in 2022. They evaluated the cost associated with the import of MCH from Saudi Arabia to Huizhou in China. The study considered the dehydrogenation and purification processes after transportation, with costs of EUR 3.46 and 4.1/kg_{H2}, respectively. These costs are unsustainable for large-scale applications, and the study identified two actions that can help to overcome such drawbacks. The first one has been introduced in Section 2.4, and it regards the high energy consumption of the dehydrogenation stage. The above analysis underlines the importance of developing catalysts for MCH dehydrogenation that remain active under milder conditions. Li et al. [145] focused on the balance of plants, proposing the integration of an endothermal catalytic stage with industrial waste heat, or in combination with high-temperature hydrogen power systems, such as those using molten carbonate fuel cell (MCFC) and solid oxide fuel cell (SOFC). The latter action is related to the scale of importation, and an increase from 10,000 tons/year to 100,000 tons/year is estimated to reduce the cost by more than 60%.

Another interesting analysis of the supply chain's impact on the final hydrogen cost was undertaken by Rasool et al. [161], which elaborates on eight different scenarios. The authors consider two alternatives for hydrogen production (alkaline and membrane), four carriers (CH_2, LH_2, CH_3OH, and NH_3), and three different export destinations from Australia (Singapore, Japan, Germany). The analysis shows the high complexity of decision-making due to the multilevel systems involved. Furthermore, the study also highlighted the impact of the parameters that can be considered decision criteria, such as the expected levelized cost of hydrogen (ELCOH) or the expected levelized cost of energy (ELCOE). Based on ELCOH, the best option is the storage of hydrogen derived from alkaline electrolyzers in NH_3, with costs of USD 8.6, 8.78, and 9.63/kg_{H2} if exported to Singapore, Japan, and Germany, respectively. On the other hand, the ELCOE implies that methanol has the best effects on the supply chain, with corresponding prices for the three destinations of USD 73.34/GJ (Singapore), 74.21/GJ (Japan), and 77.65/GJ (Germany).

4. Conclusions and Perspectives

This review critically discusses the most promising hydrogen carriers for hydrogen storage, which are essential to the transition towards cleaner and more sustainable energy production. For each hydrogen carrier considered, the state-of-the-art for its production and final release has been discussed and compared with the latest and most innovative approaches proposed in the literature. The current research frontiers indicate that ammonia, metal hydrides and carbon-based compounds (methanol, formic acid, and LOHC) can act as hydrogen carriers, allowing the storage of hydrogen under milder conditions than conventional compressed and liquefied hydrogen. Nevertheless, the analysis also highlights that, although promising results have been reached in the last few years, more effort will be required in the future to overcome the issues that remain unsolved.

From a scientific point of view, the first problem that researchers must face is related to catalyst formulation for the hydrogenation and dehydrogenation stages. The next-gen catalytic materials must be able to operate under milder conditions (pressure and temperature) than state-of-the-art materials, and should contain lower quantities of PGM elements, which will reduce their price. For carbon-based hydrogen carriers, integration with CCS technologies will be fundamental, as will be considering the possibility of recovering and reusing the unsaturated form of LOHC after hydrogen release. Also, we must improve metal hydrides' recyclability, and make hydrogen from them release faster at temperatures below 85 °C.

These scientific developments must be coupled with techno-economic analyses in order to reach the deeper market penetration of hydrogen technologies. In Section 3, it is evident that the hydrogen economy is dependent on many factors, and some of these are not related to scientific knowledge. A strong influence in the next few years will be exhibited by national and transnational policies and decision-makers' actions, which will drive investments and infrastructure development, thus determining the fate of hydrogen carriers.

Author Contributions: Conceptualization, D.C., L.M. and A.B.; investigation: D.C., D.B. and M.R.; writing—original draft preparation: D.C., D.B. and M.R.; project administration: L.M. and A.B. All authors have read and agreed to the published version of the manuscript.

Funding: This work was partially supported by the Project "PNRR programme project NEST-NETWORK 4 ENERGY SUSTAINABLE TRANSITION, Spoke 4" (PE0000021).

Data Availability Statement: All necessary data in this review are included in the paper.

Conflicts of Interest: The authors declare no conflict of interest.

List of Abbreviations

18H-DBT	perhydrodibenzyltoluene
AC	active carbon
ACC	activated carbon cloth
AWEs	alkaline water electrolyzers
BNZ	benzene
CAPEX	capital expenditure
CCS	carbon capture and storage
CH_2	compressed hydrogen
CHX	cyclohexane
CNTs	carbonanotubes
CRW	critical raw materials
DBT	dibenzyltoluene
DCL	decalin
DMSO	dimethyl sulfoxide
ELCOE	expected levelized cost of energy
ELCOH	expected levelized cost of hydrogen
FA	formic acid
FE	Faradaic efficiency

GHG	greenhouse gases
HB	Haber–Bosch
HER	hydrogen evolution reaction
ICE	internal combustion engine
LH_2	liquefied hydrogen
LNG	liquefied natural gas
LOHC	liquid organic hydrogen carrier
MCFC	molten carbonate fuel cell
MCH	methylcyclohexane
MH	metal hydride
NPT	naphthalene
OPEX	operational expenditure
P2X	power-to-X
PEMWEs	polymer electrolyte membrane water electrolyzers
PGM	platinum-group metals
RES	renewable energy source
SAC	single atom catalyst
SOECs	solid oxide electrolyzers cells
SHE	standard hydrogen electrode
SRM	steam reforming of methanol
TOF	turnover frequency
TOL	toluene

References

1. Shiva Kumar, S.; Lim, H. An overview of water electrolysis technologies for green hydrogen production. *Energy Rep.* **2022**, *8*, 13793–13813. [CrossRef]
2. Wang, X.; Star, A.G.; Ahluwalia, R.K. Performance of Polymer Electrolyte Membrane Water Electrolysis Systems: Configuration, Stack Materials, Turndown and Efficiency. *Energies* **2023**, *16*, 4964. [CrossRef]
3. Shiva Kumar, S.; Himabindu, V. Hydrogen production by PEM water electrolysis—A review. *Mater. Sci. Energy Technol.* **2019**, *2*, 442–454. [CrossRef]
4. Fan, L.; Tu, Z.; Chan, S.H. Recent development of hydrogen and fuel cell technologies: A review. *Energy Rep.* **2021**, *7*, 8421–8446. [CrossRef]
5. Cigolotti, V.; Genovese, M.; Fragiacomo, P. Comprehensive Review on Fuel Cell Technology for Stationary Applications as Sustainable and Efficient Poly-Generation Energy Systems. *Energies* **2021**, *14*, 4963. [CrossRef]
6. Tian, Y.; Abhishek, N.; Yang, C.; Yang, R.; Choi, S.; Chi, B.; Pu, J.; Ling, Y.; Irvine, J.T.S.; Kim, G.; et al. Progress and potential for symmetrical solid oxide electrolysis cells. *Matter* **2022**, *5*, 482–514. [CrossRef]
7. Kim-Lohsoontorn, P.; Prasopchokkul, P.; Wongmaek, A.; Temluxame, P.; Visvanichkul, R.; Bairak, S.; Nuengjumnong, N. Durability and Degradation Issues in Solid Oxide Electrolysis Cells. In *High Temperature Electrolysis*; Laguna-Bercero, M.A., Ed.; Springer International Publishing: Cham, Switzerland, 2023; pp. 277–312.
8. Pareek, A.; Dom, R.; Gupta, J.; Chandran, J.; Adepu, V.; Borse, P.H. Insights into renewable hydrogen energy: Recent advances and prospects. *Mater. Sci. Energy Technol.* **2020**, *3*, 319–327. [CrossRef]
9. Megía, P.J.; Vizcaíno, A.J.; Calles, J.A.; Carrero, A. Hydrogen Production Technologies: From Fossil Fuels toward Renewable Sources. A Mini Review. *Energy Fuels* **2021**, *35*, 16403–16415. [CrossRef]
10. Dash, S.K.; Chakraborty, S.; Elangovan, D.A. Brief Review of Hydrogen Production Methods and Their Challenges. *Energies* **2023**, *16*, 1141. [CrossRef]
11. Yan, H.; Zhang, W.; Kang, J.; Yuan, T. The Necessity and Feasibility of Hydrogen Storage for Large-Scale, Long-Term Energy Storage in the New Power System in China. *Energies* **2023**, *16*, 4837. [CrossRef]
12. Osman, A.I.; Mehta, N.; Elgarahy, A.M.; Hefny, M.; Al-Hinai, A.; Al-Muhtaseb, A.a.H.; Rooney, D.W. Hydrogen production, storage, utilisation and environmental impacts: A review. *Environ. Chem. Lett.* **2022**, *20*, 153–188. [CrossRef]
13. Moradi, R.; Groth, K.M. Hydrogen storage and delivery: Review of the state of the art technologies and risk and reliability analysis. *Int. J. Hydrogen Energy* **2019**, *44*, 12254–12269. [CrossRef]
14. Li, J.-Q.; Li, J.-C.; Park, K.; Jang, S.-J.; Kwon, J.-T. An Analysis on the Compressed Hydrogen Storage System for the Fast-Filling Process of Hydrogen Gas at the Pressure of 82 MPa. *Energies* **2021**, *14*, 2635. [CrossRef]
15. Elberry, A.M.; Thakur, J.; Santasalo-Aarnio, A.; Larmi, M. Large-scale compressed hydrogen storage as part of renewable electricity storage systems. *Int. J. Hydrogen Energy* **2021**, *46*, 15671–15690. [CrossRef]
16. Yue, M.; Lambert, H.; Pahon, E.; Roche, R.; Jemei, S.; Hissel, D. Hydrogen energy systems: A critical review of technologies, applications, trends and challenges. *Renew. Sustain. Energy Rev.* **2021**, *146*, 111180. [CrossRef]
17. Abohamzeh, E.; Salehi, F.; Sheikholeslami, M.; Abbassi, R.; Khan, F. Review of hydrogen safety during storage, transmission, and applications processes. *J. Loss Prev. Process Ind.* **2021**, *72*, 104569. [CrossRef]

18. Bockris, J.O.M. The hydrogen economy: Its history. *Int. J. Hydrogen Energy* **2013**, *38*, 2579–2588. [CrossRef]
19. Lee, W.H.; Kim, K.; Koh, J.H.; Lee, D.K.; Won, D.H.; Oh, H.-S.; Lee, U.; Min, B.K. The green-ol (green-alcohol) economy. *Nano Energy* **2023**, *110*, 108373. [CrossRef]
20. Zivar, D.; Kumar, S.; Foroozesh, J. Underground hydrogen storage: A comprehensive review. *Int. J. Hydrogen Energy* **2021**, *46*, 23436–23462. [CrossRef]
21. Uliasz-Misiak, B.; Lewandowska-Śmierzchalska, J.; Matuła, R.; Tarkowski, R. Prospects for the Implementation of Underground Hydrogen Storage in the EU. *Energies* **2022**, *15*, 9535. [CrossRef]
22. Zohuri, B. Cryogenics and Liquid Hydrogen Storage. In *Hydrogen Energy: Challenges and Solutions for a Cleaner Future*; Zohuri, B., Ed.; Springer International Publishing: Cham, Switzerland, 2019; pp. 121–139.
23. Tarasov, B.P.; Fursikov, P.V.; Volodin, A.A.; Bocharnikov, M.S.; Shimkus, Y.Y.; Kashin, A.M.; Yartys, V.A.; Chidziva, S.; Pasupathi, S.; Lototskyy, M.V.; et al. Metal hydride hydrogen storage and compression systems for energy storage technologies. *Int. J. Hydrogen Energy* **2021**, *46*, 13647–13657. [CrossRef]
24. Ali, N.A.; Ismail, M. Advanced hydrogen storage of the Mg–Na–Al system: A review. *J. Magnes. Alloys* **2021**, *9*, 1111–1122. [CrossRef]
25. Van Hoecke, L.; Laffineur, L.; Campe, R.; Perreault, P.; Verbruggen, S.W.; Lenaerts, S. Challenges in the use of hydrogen for maritime applications. *Energy Environ. Sci.* **2021**, *14*, 815–843. [CrossRef]
26. Ghorbani, B.; Zendehboudi, S.; Saady, N.M.C.; Duan, X.; Albayati, T.M. Strategies To Improve the Performance of Hydrogen Storage Systems by Liquefaction Methods: A Comprehensive Review. *ACS Omega* **2023**, *8*, 18358–18399. [CrossRef] [PubMed]
27. Wan, Z.; Tao, Y.; Shao, J.; Zhang, Y.; You, H. Ammonia as an effective hydrogen carrier and a clean fuel for solid oxide fuel cells. *Energy Convers. Manag.* **2021**, *228*, 113729. [CrossRef]
28. Salmon, N.; Bañares-Alcántara, R. Green ammonia as a spatial energy vector: A review. *Sustain. Energy Fuels* **2021**, *5*, 2814–2839. [CrossRef]
29. Chang, F.; Gao, W.; Guo, J.; Chen, P. Emerging Materials and Methods toward Ammonia-Based Energy Storage and Conversion. *Adv. Mater.* **2021**, *33*, 2005721. [CrossRef]
30. Schorn, F.; Breuer, J.L.; Samsun, R.C.; Schnorbus, T.; Heuser, B.; Peters, R.; Stolten, D. Methanol as a renewable energy carrier: An assessment of production and transportation costs for selected global locations. *Adv. Appl. Energy* **2021**, *3*, 100050. [CrossRef]
31. Pethaiah, S.S.; Sadasivuni, K.K.; Jayakumar, A.; Ponnamma, D.; Tiwary, C.S.; Sasikumar, G. Methanol Electrolysis for Hydrogen Production Using Polymer Electrolyte Membrane: A Mini-Review. *Energies* **2020**, *13*, 5879. [CrossRef]
32. Garcia, G.; Arriola, E.; Chen, W.-H.; De Luna, M.D. A comprehensive review of hydrogen production from methanol thermochemical conversion for sustainability. *Energy* **2021**, *217*, 119384. [CrossRef]
33. Dutta, I.; Chatterjee, S.; Cheng, H.; Parsapur, R.K.; Liu, Z.; Li, Z.; Ye, E.; Kawanami, H.; Low, J.S.C.; Lai, Z.; et al. Formic Acid to Power towards Low-Carbon Economy. *Adv. Energy Mater.* **2022**, *12*, 2103799. [CrossRef]
34. Chatterjee, S.; Dutta, I.; Lum, Y.; Lai, Z.; Huang, K.-W. Enabling storage and utilization of low-carbon electricity: Power to formic acid. *Energy Environ. Sci.* **2021**, *14*, 1194–1246. [CrossRef]
35. Salman, M.S.; Rambhujun, N.; Pratthana, C.; Srivastava, K.; Aguey-Zinsou, K.-F. Catalysis in Liquid Organic Hydrogen Storage: Recent Advances, Challenges, and Perspectives. *Ind. Eng. Chem. Res.* **2022**, *61*, 6067–6105. [CrossRef]
36. Perreault, P.; Van Hoecke, L.; Pourfallah, H.; Kummamuru, N.B.; Boruntea, C.-R.; Preuster, P. Critical challenges towards the commercial rollouts of a LOHC-based H_2 economy. *Curr. Opin. Green Sustain. Chem.* **2023**, *41*, 100836. [CrossRef]
37. Aakko-Saksa, P.T.; Cook, C.; Kiviaho, J.; Repo, T. Liquid organic hydrogen carriers for transportation and storing of renewable energy—Review and discussion. *J. Power Sources* **2018**, *396*, 803–823. [CrossRef]
38. Aziz, M.; Wijayanta, A.T.; Nandiyanto, A.B.D. Ammonia as Effective Hydrogen Storage: A Review on Production, Storage and Utilization. *Energies* **2020**, *13*, 3062. [CrossRef]
39. Ishaq, H.; Dincer, I.; Crawford, C. A review on hydrogen production and utilization: Challenges and opportunities. *Int. J. Hydrogen Energy* **2022**, *47*, 26238–26264. [CrossRef]
40. Agyekum, E.B.; Nutakor, C.; Agwa, A.M.; Kamel, S.A. Critical Review of Renewable Hydrogen Production Methods: Factors Affecting Their Scale-Up and Its Role in Future Energy Generation. *Membranes* **2022**, *12*, 173. [CrossRef]
41. Ghoreishian, S.M.; Shariati, K.; Huh, Y.S.; Lauterbach, J. Recent advances in ammonia synthesis over ruthenium single-atom-embedded catalysts: A focused review. *Chem. Eng. J.* **2023**, *467*, 143533. [CrossRef]
42. El-Shafie, M.; Kambara, S. Recent advances in ammonia synthesis technologies: Toward future zero carbon emissions. *Int. J. Hydrogen Energy* **2023**, *48*, 11237–11273. [CrossRef]
43. Humphreys, J.; Lan, R.; Tao, S. Development and Recent Progress on Ammonia Synthesis Catalysts for Haber–Bosch Process. *Adv. Energy Sustain. Res.* **2021**, *2*, 2000043. [CrossRef]
44. Attari Moghaddam, A.; Krewer, U. Poisoning of Ammonia Synthesis Catalyst Considering Off-Design Feed Compositions. *Catalysts* **2020**, *10*, 1225. [CrossRef]
45. Oshikiri, T.; Ueno, K.; Misawa, H. Plasmon-Induced Ammonia Synthesis through Nitrogen Photofixation with Visible Light Irradiation. *Angew. Chem. Int. Ed.* **2014**, *53*, 9802–9805. [CrossRef] [PubMed]

46. Gao, W.; Wang, Q.; Guan, Y.; Yan, H.; Guo, J.; Chen, P. Barium hydride activates Ni for ammonia synthesis catalysis. *Faraday Discuss.* **2023**, *243*, 27–37. [CrossRef]
47. Sato, K.; Miyahara, S.-i.; Tsujimaru, K.; Wada, Y.; Toriyama, T.; Yamamoto, T.; Matsumura, S.; Inazu, K.; Mohri, H.; Iwasa, T.; et al. Barium Oxide Encapsulating Cobalt Nanoparticles Supported on Magnesium Oxide: Active Non-Noble Metal Catalysts for Ammonia Synthesis under Mild Reaction Conditions. *ACS Catal.* **2021**, *11*, 13050–13061. [CrossRef]
48. Nazemi, M.; Ou, P.; Alabbady, A.; Soule, L.; Liu, A.; Song, J.; Sulchek, T.A.; Liu, M.; El-Sayed, M.A. Electrosynthesis of Ammonia Using Porous Bimetallic Pd–Ag Nanocatalysts in Liquid- and Gas-Phase Systems. *ACS Catal.* **2020**, *10*, 10197–10206. [CrossRef]
49. Xu, G.; Liu, R.; Wang, J. Electrochemical synthesis of ammonia using a cell with a Nafion membrane and $SmFe_{0.7}Cu_{0.3-x}Ni_xO_3$ (x = 0 − 0.3) cathode at atmospheric pressure and lower temperature. *Sci. China Ser. B Chem.* **2009**, *52*, 1171–1175. [CrossRef]
50. Wang, Y.; Yu, W.; Li, X.; Yu, J.; Zhou, W. Electrocatalytic reduction of nitrogenous pollutants to ammonia. *Chem. Eng. J.* **2023**, *469*, 143889. [CrossRef]
51. Zhou, Y.; Zhu, Y.; Zhu, J.; Li, C.; Chen, G. A Comprehensive Review on Wastewater Nitrogen Removal and Its Recovery Processes. *Int. J. Environ. Res. Public Health* **2023**, *20*, 3429. [CrossRef]
52. Yao, J.; Mei, Y.; Yuan, T.; Chen, J.; Pan, H.; Wang, J. Electrochemical removal of nitrate from wastewater with a Ti cathode and Pt anode for high efficiency and N2 selectivity. *J. Electroanal. Chem.* **2021**, *882*, 115019. [CrossRef]
53. Song, Z.; Liu, Y.; Zhong, Y.; Guo, Q.; Zeng, J.; Geng, Z. Efficient Electroreduction of Nitrate into Ammonia at Ultralow Concentrations Via an Enrichment Effect. *Adv. Mater.* **2022**, *34*, 2204306. [CrossRef] [PubMed]
54. Kim, K.; Zagalskaya, A.; Ng, J.L.; Hong, J.; Alexandrov, V.; Pham, T.A.; Su, X. Coupling nitrate capture with ammonia production through bifunctional redox-electrodes. *Nat. Commun.* **2023**, *14*, 823. [CrossRef] [PubMed]
55. Ke, Z.; He, D.; Yan, X.; Hu, W.; Williams, N.; Kang, H.; Pan, X.; Huang, J.; Gu, J.; Xiao, X. Selective NOx– Electroreduction to Ammonia on Isolated Ru Sites. *ACS Nano* **2023**, *17*, 3483–3491. [CrossRef] [PubMed]
56. Cheon, S.; Kim, W.J.; Kim, D.Y.; Kwon, Y.; Han, J.-I. Electro-synthesis of Ammonia from Dilute Nitric Oxide on a Gas Diffusion Electrode. *ACS Energy Lett.* **2022**, *7*, 958–965. [CrossRef]
57. Kwon, Y.-i.; Kim, S.K.; Kim, Y.B.; Son, S.J.; Nam, G.D.; Park, H.J.; Cho, W.-C.; Yoon, H.C.; Joo, J.H. Nitric oxide utilization for ammonia production using solid electrolysis cell at atmospheric pressure. *ACS Energy Lett.* **2021**, *6*, 4165–4172. [CrossRef]
58. Sun, S.; Jiang, Q.; Zhao, D.; Cao, T.; Sha, H.; Zhang, C.; Song, H.; Da, Z. Ammonia as hydrogen carrier: Advances in ammonia decomposition catalysts for promising hydrogen production. *Renew. Sustain. Energy Rev.* **2022**, *169*, 112918. [CrossRef]
59. Lu, B.; Li, L.; Ren, M.; Liu, Y.; Zhang, Y.; Xu, X.; Wang, X.; Qiu, H. Ammonia decomposition over iron-based catalyst: Exploring the hidden active phase. *Appl. Catal. B Environ.* **2022**, *314*, 121475. [CrossRef]
60. Chen, C.; Wu, K.; Ren, H.; Zhou, C.; Luo, Y.; Lin, L.; Au, C.; Jiang, L. Ru-Based Catalysts for Ammonia Decomposition: A Mini-Review. *Energy Fuels* **2021**, *35*, 11693–11706. [CrossRef]
61. Astruc, D. Introduction: Nanoparticles in Catalysis. *Chem. Rev.* **2020**, *120*, 461–463. [CrossRef]
62. Hill, A.K.; Torrente-Murciano, L. In-situ H_2 production via low temperature decomposition of ammonia: Insights into the role of cesium as a promoter. *Int. J. Hydrogen Energy* **2014**, *39*, 7646–7654. [CrossRef]
63. Lezcano, G.; Realpe, N.; Kulkarni, S.R.; Sayas, S.; Cerrillo, J.; Morlanes, N.; Mohamed, H.O.; Velisoju, V.K.; Aldilajan, R.F.; Katikaneni, S.P.; et al. Unraveling the promoter role of Ba in Co–Ce catalysts for ammonia decomposition using microkinetic modeling. *Chem. Eng. J.* **2023**, *471*, 144623. [CrossRef]
64. Sayas, S.; Morlanés, N.; Katikaneni, S.P.; Harale, A.; Solami, B.; Gascon, J. High pressure ammonia decomposition on Ru–K/CaO catalysts. *Catal. Sci. Technol.* **2020**, *10*, 5027–5035. [CrossRef]
65. Lee, H.J.; Park, E.D. Ammonia Decomposition over Ru/SiO_2 Catalysts. *Catalysts* **2022**, *12*, 1203. [CrossRef]
66. Feng, J.; Liu, L.; Ju, X.; Wang, J.; Zhang, X.; He, T.; Chen, P. Highly Dispersed Ruthenium Nanoparticles on Y_2O_3 as Superior Catalyst for Ammonia Decomposition. *ChemCatChem* **2021**, *13*, 1552–1558. [CrossRef]
67. Zhang, X.; Liu, L.; Feng, J.; Ju, X.; Wang, J.; He, T.; Chen, P. Metal–support interaction-modulated catalytic activity of Ru nanoparticles on Sm_2O_3 for efficient ammonia decomposition. *Catal. Sci. Technol.* **2021**, *11*, 2915–2923. [CrossRef]
68. Lucentini, I.; Casanovas, A.; Llorca, J. Catalytic ammonia decomposition for hydrogen production on Ni, Ru and NiRu supported on CeO_2. *Int. J. Hydrogen Energy* **2019**, *44*, 12693–12707. [CrossRef]
69. Cao, C.-F.; Wu, K.; Zhou, C.; Yao, Y.-H.; Luo, Y.; Chen, C.-Q.; Lin, L.; Jiang, L. Electronic metal-support interaction enhanced ammonia decomposition efficiency of perovskite oxide supported ruthenium. *Chem. Eng. Sci.* **2022**, *257*, 117719. [CrossRef]
70. Chen, Y.-L.; Juang, C.-F.; Chen, Y.-C. The Effects of Promoter Cs Loading on the Hydrogen Production from Ammonia Decomposition Using Ru/C Catalyst in a Fixed-Bed Reactor. *Catalysts* **2021**, *11*, 321. [CrossRef]
71. Akarçay, Ö.; Kurtoğlu, S.F.; Uzun, A. Ammonia decomposition on a highly-dispersed carbon-embedded iron catalyst derived from Fe-BTC: Stable and high performance at relatively low temperatures. *Int. J. Hydrogen Energy* **2020**, *45*, 28664–28681. [CrossRef]
72. Zhou, S.; Lin, S.; Guo, H. First-Principles Insights into Ammonia Decomposition Catalyzed by Ru Clusters Anchored on Carbon Nanotubes: Size Dependence and Interfacial Effects. *J. Phys. Chem. C* **2018**, *122*, 9091–9100. [CrossRef]
73. Rangraz, Y.; Heravi, M.M. Recent advances in metal-free heteroatom-doped carbon heterogonous catalysts. *RSC Adv.* **2021**, *11*, 23725–23778. [CrossRef] [PubMed]
74. Olah, G.A. Beyond Oil and Gas: The Methanol Economy. *Angew. Chem. Int. Ed.* **2005**, *44*, 2636–2639. [CrossRef] [PubMed]

75. Bellotti, D.; Rivarolo, M.; Magistri, L.; Massardo, A.F. Feasibility study of methanol production plant from hydrogen and captured carbon dioxide. *J. CO2 Util.* **2017**, *21*, 132–138. [CrossRef]
76. Palone, O.; Gagliardi, G.G.; Mechelli, M.; Cedola, L.; Borello, D. Techno-economic analysis of sustainable methanol and ammonia production by chemical looping hydrogen generation from waste plastic. *Energy Convers. Manag.* **2023**, *292*, 117389. [CrossRef]
77. Zhang, F.; Xu, X.; Qiu, Z.; Feng, B.; Liu, Y.; Xing, A.; Fan, M. Improved methanol synthesis performance of $Cu/ZnO/Al_2O_3$ catalyst by controlling its precursor structure. *Green Energy Environ.* **2022**, *7*, 772–781. [CrossRef]
78. Niermann, M.; Beckendorff, A.; Kaltschmitt, M.; Bonhoff, K. Liquid Organic Hydrogen Carrier (LOHC)—Assessment based on chemical and economic properties. *Int. J. Hydrogen Energy* **2019**, *44*, 6631–6654. [CrossRef]
79. Shen, W.-J.; Jun, K.-W.; Choi, H.-S.; Lee, K.-W. Thermodynamic investigation of methanol and dimethyl ether synthesis from CO_2 Hydrogenation. *Korean J. Chem. Eng.* **2000**, *17*, 210–216. [CrossRef]
80. Marlin, D.S.; Sarron, E.; Sigurbjörnsson, Ó. Process Advantages of Direct CO_2 to Methanol Synthesis. *Front. Chem.* **2018**, *6*, 446. [CrossRef]
81. Wiranarongkorn, K.; Eamsiri, K.; Chen, Y.-S.; Arpornwichanop, A. A comprehensive review of electrochemical reduction of CO_2 to methanol: Technical and design aspects. *J. CO2 Util.* **2023**, *71*, 102477. [CrossRef]
82. Liu, Y.; Li, F.; Zhang, X.; Ji, X. Recent progress on electrochemical reduction of CO_2 to methanol. *Curr. Opin. Green Sustain. Chem.* **2020**, *23*, 10–17. [CrossRef]
83. Albo, J.; Sáez, A.; Solla-Gullón, J.; Montiel, V.; Irabien, A. Production of methanol from CO_2 electroreduction at Cu_2O and Cu_2O/ZnO-based electrodes in aqueous solution. *Appl. Catal. B Environ.* **2015**, *176–177*, 709–717. [CrossRef]
84. Guo, W.; Liu, S.; Tan, X.; Wu, R.; Yan, X.; Chen, C.; Zhu, Q.; Zheng, L.; Ma, J.; Zhang, J.; et al. Highly Efficient CO_2 Electroreduction to Methanol through Atomically Dispersed Sn Coupled with Defective CuO Catalysts. *Angew. Chem. Int. Ed.* **2021**, *60*, 21979–21987. [CrossRef] [PubMed]
85. Huang, W.; Yuan, G. A composite heterogeneous catalyst C-Py-Sn-Zn for selective electrochemical reduction of CO_2 to methanol. *Electrochem. Commun.* **2020**, *118*, 106789. [CrossRef]
86. Bagchi, D.; Raj, J.; Singh, A.K.; Cherevotan, A.; Roy, S.; Manoj, K.S.; Vinod, C.P.; Peter, S.C. Structure-Tailored Surface Oxide on Cu–Ga Intermetallics Enhances CO_2 Reduction Selectivity to Methanol at Ultralow Potential. *Adv. Mater.* **2022**, *34*, 2109426. [CrossRef] [PubMed]
87. Zuo, L.; Yu, S.; Zhang, R.; Li, H.; Wu, Y.; Abiev, R.; Sun, Z.; Sun, Z. Tunning Pd–Cu-based catalytic oxygen carrier for intensifying low-temperature methanol reforming. *J. Clean. Prod.* **2023**, *410*, 137212. [CrossRef]
88. Li, D.; Xu, F.; Tang, X.; Dai, S.; Pu, T.; Liu, X.; Tian, P.; Xuan, F.; Xu, Z.; Wachs, I.E.; et al. Induced activation of the commercial $Cu/ZnO/Al_2O_3$ catalyst for the steam reforming of methanol. *Nat. Catal.* **2022**, *5*, 99–108. [CrossRef]
89. Cheng, Z.; Zhou, W.; Lan, G.; Sun, X.; Wang, X.; Jiang, C.; Li, Y. High-performance $Cu/ZnO/Al_2O_3$ catalysts for methanol steam reforming with enhanced Cu-ZnO synergy effect via magnesium assisted strategy. *J. Energy Chem.* **2021**, *63*, 550–557. [CrossRef]
90. Yang, W.-W.; Ma, X.; Tang, X.-Y.; Dou, P.-Y.; Yang, Y.-J.; He, Y.-L. Review on developments of catalytic system for methanol steam reforming from the perspective of energy-mass conversion. *Fuel* **2023**, *345*, 128234. [CrossRef]
91. Ding, Y.; Zhang, T.; Ge, Z.; Li, P.; Shen, Y. High-efficiency steam reforming of methanol on the surface of a recyclable NiO/NaF catalyst for hydrogen production. *Compos. Part B Eng.* **2022**, *243*, 110113. [CrossRef]
92. Tanaka, Y.; Utaka, T.; Kikuchi, R.; Takeguchi, T.; Sasaki, K.; Eguchi, K. Water gas shift reaction for the reformed fuels over Cu/MnO catalysts prepared via spinel-type oxide. *J. Catal.* **2003**, *215*, 271–278. [CrossRef]
93. Yang, X.; Bulushev, D.A.; Yang, J.; Zhang, Q. New Liquid Chemical Hydrogen Storage Technology. *Energies* **2022**, *15*, 6360. [CrossRef]
94. Wei, D.; Shi, X.; Qu, R.; Junge, K.; Junge, H.; Beller, M. Toward a Hydrogen Economy: Development of Heterogeneous Catalysts for Chemical Hydrogen Storage and Release Reactions. *ACS Energy Lett.* **2022**, *7*, 3734–3752. [CrossRef]
95. Kim, C.; Lee, Y.; Kim, K.; Lee, U. Implementation of Formic Acid as a Liquid Organic Hydrogen Carrier (LOHC): Techno-Economic Analysis and Life Cycle Assessment of Formic Acid Produced via CO_2 Utilization. *Catalysts* **2022**, *12*, 1113. [CrossRef]
96. Hafeez, S.; Harkou, E.; Spanou, A.; Al-Salem, S.M.; Villa, A.; Dimitratos, N.; Manos, G.; Constantinou, A. Review on recent progress and reactor set-ups for hydrogen production from formic acid decomposition. *Mater. Today Chem.* **2022**, *26*, 101120. [CrossRef]
97. Sordakis, K.; Tang, C.; Vogt, L.K.; Junge, H.; Dyson, P.J.; Beller, M.; Laurenczy, G. Homogeneous Catalysis for Sustainable Hydrogen Storage in Formic Acid and Alcohols. *Chem. Rev.* **2018**, *118*, 372–433. [CrossRef]
98. Yadav, M.; Xu, Q. Liquid-phase chemical hydrogen storage materials. *Energy Environ. Sci.* **2012**, *5*, 9698–9725. [CrossRef]
99. Junge Puring, K.; Evers, O.; Prokein, M.; Siegmund, D.; Scholten, F.; Mölders, N.; Renner, M.; Roldan Cuenya, B.; Petermann, M.; Weidner, E.; et al. Assessing the Influence of Supercritical Carbon Dioxide on the Electrochemical Reduction to Formic Acid Using Carbon-Supported Copper Catalysts. *ACS Catal.* **2020**, *10*, 12783–12789. [CrossRef]
100. Wasik, D.O.; Martín-Calvo, A.; Gutiérrez-Sevillano, J.J.; Dubbeldam, D.; Vlugt, T.J.H.; Calero, S. Enhancement of formic acid production from carbon dioxide hydrogenation using metal-organic frameworks: Monte Carlo simulation study. *Chem. Eng. J.* **2023**, *467*, 143432. [CrossRef]

101. Bulushev, D.A. Progress in Catalytic Hydrogen Production from Formic Acid over Supported Metal Complexes. *Energies* **2021**, *14*, 1334. [CrossRef]
102. Onishi, N.; Iguchi, M.; Yang, X.; Kanega, R.; Kawanami, H.; Xu, Q.; Himeda, Y. Development of Effective Catalysts for Hydrogen Storage Technology Using Formic Acid. *Adv. Energy Mater.* **2019**, *9*, 1801275. [CrossRef]
103. Fellay, C.; Dyson, P.J.; Laurenczy, G. A Viable Hydrogen-Storage System Based On Selective Formic Acid Decomposition with a Ruthenium Catalyst. *Angew. Chem. Int. Ed.* **2008**, *47*, 3966–3968. [CrossRef] [PubMed]
104. Wang, Q.; Tsumori, N.; Kitta, M.; Xu, Q. Fast Dehydrogenation of Formic Acid over Palladium Nanoparticles Immobilized in Nitrogen-Doped Hierarchically Porous Carbon. *ACS Catal.* **2018**, *8*, 12041–12045. [CrossRef]
105. Farajzadeh, M.; Alamgholiloo, H.; Nasibipour, F.; Banaei, R.; Rostamnia, S. Anchoring Pd-nanoparticles on dithiocarbamate-functionalized SBA-15 for hydrogen generation from formic acid. *Sci. Rep.* **2020**, *10*, 18188. [CrossRef]
106. Al-Nayili, A.; Majdi, H.S.; Albayati, T.M.; Saady, N.M.C. Formic Acid Dehydrogenation Using Noble-Metal Nanoheterogeneous Catalysts: Towards Sustainable Hydrogen-Based Energy. *Catalysts* **2022**, *12*, 324. [CrossRef]
107. García, A.; Marín, P.; Ordóñez, S. Hydrogenation of liquid organic hydrogen carriers: Process scale-up, economic analysis and optimization. *Int. J. Hydrogen Energy* **2023**, *in press*. [CrossRef]
108. Chu, C.; Wu, K.; Luo, B.; Cao, Q.; Zhang, H. Hydrogen storage by liquid organic hydrogen carriers: Catalyst, renewable carrier, and technology—A review. *Carbon Resour. Convers.* **2023**, *6*, 334–351. [CrossRef]
109. Bianchini, C.; Meli, A.; Vizza, F. Hydrogenation of Arenes and Heteroaromatics. In *The Handbook of Homogeneous Hydrogenation*; Wiley: Hoboken, NJ, USA, 2006; pp. 455–488.
110. Wang, J.; Shi, J.; Wang, S.; Fan, S.; Guo, A.; Wang, Z.; Liu, H. Nitrogen-doped carbon supported PtPd alloy nanoparticles exhibiting high catalytic activity for cyclohexane dehydrogenation under low temperatures. *Fuel* **2023**, *345*, 128266. [CrossRef]
111. Chen, L.; Verma, P.; Hou, K.; Qi, Z.; Zhang, S.; Liu, Y.-S.; Guo, J.; Stavila, V.; Allendorf, M.D.; Zheng, L.; et al. Reversible dehydrogenation and rehydrogenation of cyclohexane and methylcyclohexane by single-site platinum catalyst. *Nat. Commun.* **2022**, *13*, 1092. [CrossRef]
112. Patil, S.P.; Pande, J.V.; Biniwale, R.B. Non-noble Ni–Cu/ACC bimetallic catalyst for dehydrogenation of liquid organic hydrides for hydrogen storage. *Int. J. Hydrogen Energy* **2013**, *38*, 15233–15241. [CrossRef]
113. Xia, Z.; Lu, H.; Liu, H.; Zhang, Z.; Chen, Y. Cyclohexane dehydrogenation over Ni-Cu/SiO_2 catalyst: Effect of copper addition. *Catal. Commun.* **2017**, *90*, 39–42. [CrossRef]
114. Obodo, K.O.; Ouma, C.N.M.; Bessarabov, D. Low-Pt-Based Sn Alloy for the Dehydrogenation of Methylcyclohexane to Toluene: A Density Functional Theory Study. *Catalysts* **2022**, *12*, 1221. [CrossRef]
115. Wang, Z.; Dong, C.; Tang, X.; Qin, X.; Liu, X.; Peng, M.; Xu, Y.; Song, C.; Zhang, J.; Liang, X.; et al. CO-tolerant RuNi/TiO_2 catalyst for the storage and purification of crude hydrogen. *Nat. Commun.* **2022**, *13*, 4404. [CrossRef] [PubMed]
116. Zhou, S.; Liu, X.; Xu, J.; Zhang, H.; Liu, X.; Li, P.; Wen, X.; Yang, Y.; Li, Y. Low-Temperature Hydrogenation of Toluene Using an Iron-Promoted Molybdenum Carbide Catalyst. *Catalysts* **2021**, *11*, 1079. [CrossRef]
117. Nagasawa, K.; Sugita, Y.; Atienza-Márquez, A.; Kuroda, Y.; Mitsushima, S. Effect of the cathode catalyst loading on mass transfer in toluene direct electrohydrogenation. *J. Electroanal. Chem.* **2023**, *938*, 117431. [CrossRef]
118. Imada, T.; Iida, Y.; Ueda, Y.; Chiku, M.; Higuchi, E.; Inoue, H. Electrochemical Toluene Hydrogenation Using Binary Platinum-Based Alloy Nanoparticle-Loaded Carbon Catalysts. *Catalysts* **2021**, *11*, 318. [CrossRef]
119. Alekseeva, M.V.; Gulyaeva, Y.K.; Bulavchenko, O.A.; Saraev, A.A.; Kremneva, A.M.; Stepanenko, S.A.; Koskin, A.P.; Kaichev, V.V.; Yakovlev, V.A. Promoting effect of Zn in high-loading Zn/Ni-SiO_2 catalysts for selective hydrogen evolution from methylcyclohexane. *Dalton Trans.* **2022**, *51*, 6068–6085. [CrossRef] [PubMed]
120. Lv, C.; Lou, P.; Chang, J.; Wang, R.; Gao, L.; Li, Y. Nickel single atoms/cerium oxide hybrid for hydrogen production via solar-heating catalytic dehydrogenation of methyl Cyclohexane. *J. Power Sources* **2023**, *559*, 232674. [CrossRef]
121. Pashchenko, D. Liquid organic hydrogen carriers (LOHCs) in the thermochemical waste heat recuperation systems: The energy and mass balances. *Int. J. Hydrogen Energy* **2022**, *47*, 28721–28729. [CrossRef]
122. Luo, M.; Wang, F.; Liu, Q.; Li, W.; Shao, C.; Liu, X.; Ai, B. Synergetic effect of Pt–Pd bimetallic nanoparticle on $MgAl_2O_4$ support in hydrogen production from decalin dehydrogenation. *React. Kinet. Mech. Catal.* **2023**. [CrossRef]
123. Peng, C.; Zhou, Z.; Fang, X.; Wang, H. Thermodynamics and kinetics insights into naphthalene hydrogenation over a Ni-Mo catalyst. *Chin. J. Chem. Eng.* **2021**, *39*, 173–182. [CrossRef]
124. Ma, Y.; Liu, J.; Chen, M.; Yang, Q.; Chen, H.; Guan, G.; Qin, Y.; Wang, T. Selective Hydrogenation of Naphthalene to Decalin Over Surface-Engineered α-MoC Based on Synergy between Pd Doping and Mo Vacancy Generation. *Adv. Funct. Mater.* **2022**, *32*, 2112435. [CrossRef]
125. Zhang, M.; Song, Q.; He, Z.; Wang, Q.; Wang, L.; Zhang, X.; Li, G. Tuning the mesopore-acid-metal balance in Pd/HY for efficient deep hydrogenation saturation of naphthalene. *Int. J. Hydrogen Energy* **2022**, *47*, 20881–20893. [CrossRef]
126. Vargas-Villagrán, H.; Ramírez-Suárez, D.; Ramírez-Muñoz, G.; Calzada, L.A.; González-García, G.; Klimova, T.E. Tuning of activity and selectivity of Ni/(Al)SBA-15 catalysts in naphthalene hydrogenation. *Catal. Today* **2021**, *360*, 27–37. [CrossRef]
127. Wang, F.; Luo, M.; Liu, Q.; Shao, C.; Yang, Z.; Liu, X.; Guo, J. Preparation of Pt/$MgAl_2O_4$ Decalin Dehydrogenation Catalyst for Chemical Hydrogen Storage Application. *Catal. Lett.* **2023**. [CrossRef]

128. Jorschick, H.; Bulgarin, A.; Alletsee, L.; Preuster, P.; Bösmann, A.; Wasserscheid, P. Charging a Liquid Organic Hydrogen Carrier with Wet Hydrogen from Electrolysis. *ACS Sustain. Chem. Eng.* **2019**, *7*, 4186–4194. [CrossRef]
129. Brückner, N.; Obesser, K.; Bösmann, A.; Teichmann, D.; Arlt, W.; Dungs, J.; Wasserscheid, P. Evaluation of Industrially Applied Heat-Transfer Fluids as Liquid Organic Hydrogen Carrier Systems. *ChemSusChem* **2014**, *7*, 229–235. [CrossRef]
130. Ali, A.; Rohini, A.K.; Lee, H.J. Dehydrogenation of perhydro-dibenzyltoluene for hydrogen production in a microchannel reactor. *Int. J. Hydrogen Energy* **2022**, *47*, 20905–20914. [CrossRef]
131. Kotowicz, J.; Uchman, W.; Jurczyk, M.; Sekret, R. Evaluation of the potential for distributed generation of green hydrogen using metal-hydride storage methods. *Appl. Energy* **2023**, *344*, 121269. [CrossRef]
132. Schneemann, A.; White, J.L.; Kang, S.; Jeong, S.; Wan, L.F.; Cho, E.S.; Heo, T.W.; Prendergast, D.; Urban, J.J.; Wood, B.C.; et al. Nanostructured Metal Hydrides for Hydrogen Storage. *Chem. Rev.* **2018**, *118*, 10775–10839. [CrossRef] [PubMed]
133. Ouyang, L.; Chen, W.; Liu, J.; Felderhoff, M.; Wang, H.; Zhu, M. Enhancing the Regeneration Process of Consumed $NaBH_4$ for Hydrogen Storage. *Adv. Energy Mater.* **2017**, *7*, 1700299. [CrossRef]
134. Ou, T.; Panizza, M.; Barbucci, A. Thermochemical recycling of hydrolyzed $NaBH_4$. Part II: Systematical study of parameters dependencies. *Int. J. Hydrogen Energy* **2013**, *38*, 15940–15945. [CrossRef]
135. Ou, T.; Giuliano, A.; Panizza, M.; Barbucci, A.; Cerisola, G. Thermochemical recycling of hydrolyzed NaBH4. Part I: In-situ and ex-situ evaluations. *Int. J. Hydrogen Energy* **2013**, *38*, 15269–15274. [CrossRef]
136. Yang, Y.; Zhang, X.; Zhang, L.; Zhang, W.; Liu, H.; Huang, Z.; Yang, L.; Gu, C.; Sun, W.; Gao, M.; et al. Recent advances in catalyst-modified Mg-based hydrogen storage materials. *J. Mater. Sci. Technol.* **2023**, *163*, 182–211. [CrossRef]
137. Dong, S.; Li, C.; Lv, E.; Wang, J.; Liu, H.; Gao, Z.; Xiong, W.; Ding, Z.; Yang, W.; Li, H. MgH_2/single-atom heterojunctions: Effective hydrogen storage materials with facile dehydrogenation. *J. Mater. Chem. A* **2022**, *10*, 19839–19851. [CrossRef]
138. Galey, B.; Auroux, A.; Sabo-Etienne, S.; Dhaher, S.; Grellier, M.; Postole, G. Improved hydrogen storage properties of Mg/MgH_2 thanks to the addition of nickel hydride complex precursors. *Int. J. Hydrogen Energy* **2019**, *44*, 28848–28862. [CrossRef]
139. Ding, Z.; Li, Y.; Yang, H.; Lu, Y.; Tan, J.; Li, J.; Li, Q.; Chen, Y.; Shaw, L.L.; Pan, F. Tailoring MgH_2 for hydrogen storage through nanoengineering and catalysis. *J. Magnes. Alloys* **2022**, *10*, 2946–2967. [CrossRef]
140. Singh, P.K.; Shinzato, K.; Gi, H.; Ichikawa, T.; Miyaoka, H. Systematic study on catalysis of group 4–6 element oxide for magnesium hydride. *J. Alloys Compd.* **2023**, *960*, 170630. [CrossRef]
141. Wagemans, R.W.P.; van Lenthe, J.H.; de Jongh, P.E.; van Dillen, A.J.; de Jong, K.P. Hydrogen Storage in Magnesium Clusters: Quantum Chemical Study. *J. Am. Chem. Soc.* **2005**, *127*, 16675–16680. [CrossRef]
142. Zhang, X.; Liu, Y.; Ren, Z.; Zhang, X.; Hu, J.; Huang, Z.; Lu, Y.; Gao, M.; Pan, H. Realizing 6.7 wt% reversible storage of hydrogen at ambient temperature with non-confined ultrafine magnesium hydrides. *Energy Environ. Sci.* **2021**, *14*, 2302–2313. [CrossRef]
143. Lee, J.-S.; Cherif, A.; Yoon, H.-J.; Seo, S.-K.; Bae, J.-E.; Shin, H.-J.; Lee, C.; Kwon, H.; Lee, C.-J. Large-scale overseas transportation of hydrogen: Comparative techno-economic and environmental investigation. *Renew. Sustain. Energy Rev.* **2022**, *165*, 112556. [CrossRef]
144. Bellotti, D.; Rivarolo, M.; Magistri, L. A comparative techno-economic and sensitivity analysis of Power-to-X processes from different energy sources. *Energy Convers. Manag.* **2022**, *260*, 115565. [CrossRef]
145. Li, L.; Vellayani Aravind, P.; Woudstra, T.; van den Broek, M. Assessing the waste heat recovery potential of liquid organic hydrogen carrier chains. *Energy Convers. Manag.* **2023**, *276*, 116555. [CrossRef]
146. Hinkley, J.T.; Heenan, A.R.; Low, A.C.S.; Watson, M. Hydrogen as an export commodity—Capital expenditure and energy evaluation of hydrogen carriers. *Int. J. Hydrogen Energy* **2022**, *47*, 35959–35975. [CrossRef]
147. Dickson, R.; Akhtar, M.S.; Abbas, A.; Park, E.D.; Liu, J. Global transportation of green hydrogen via liquid carriers: Economic and environmental sustainability analysis, policy implications, and future directions. *Green Chem.* **2022**, *24*, 8484–8493. [CrossRef]
148. Pérez-Fortes, M.; Schöneberger, J.C.; Boulamanti, A.; Tzimas, E. Methanol synthesis using captured CO_2 as raw material: Techno-economic and environmental assessment. *Appl. Energy* **2016**, *161*, 718–732. [CrossRef]
149. Cui, J.; Aziz, M. Techno-economic analysis of hydrogen transportation infrastructure using ammonia and methanol. *Int. J. Hydrogen Energy* **2023**, *48*, 15737–15747. [CrossRef]
150. Bellotti, D.; Sorce, A.; Rivarolo, M.; Magistri, L. Techno-economic analysis for the integration of a power to fuel system with a CCS coal power plant. *J. CO2 Util.* **2019**, *33*, 262–272. [CrossRef]
151. Kistner, L.; Bensmann, A.; Minke, C.; Hanke-Rauschenbach, R. Comprehensive techno-economic assessment of power technologies and synthetic fuels under discussion for ship applications. *Renew. Sustain. Energy Rev.* **2023**, *183*, 113459. [CrossRef]
152. Rivarolo, M.; Rattazzi, D.; Magistri, L.; Massardo, A.F. Multi-criteria comparison of power generation and fuel storage solutions for maritime application. *Energy Convers. Manag.* **2021**, *244*, 114506. [CrossRef]
153. Xu, Z.; Zhao, N.; Hillmansen, S.; Roberts, C.; Yan, Y. Techno-Economic Analysis of Hydrogen Storage Technologies for Railway Engineering: A Review. *Energies* **2022**, *15*, 6467. [CrossRef]
154. Ibagon, N.; Muñoz, P.; Díaz, V.; Teliz, E.; Correa, G. Techno-economic analysis for off-grid green hydrogen production in Uruguay. *J. Energy Storage* **2023**, *67*, 107604. [CrossRef]
155. Godinho, J.; Hoefnagels, R.; Braz, C.G.; Sousa, A.M.; Granjo, J.F.O. An economic and greenhouse gas footprint assessment of international maritime transportation of hydrogen using liquid organic hydrogen carriers. *Energy* **2023**, *278*, 127673. [CrossRef]

156. Cavo, M.; Rivarolo, M.; Gini, L.; Magistri, L. An advanced control method for fuel cells—Metal hydrides thermal management on the first Italian hydrogen propulsion ship. *Int. J. Hydrogen Energy* **2023**, *48*, 20923–20934. [CrossRef]
157. Schöne, N.; Dumitrescu, R.; Heinz, B. Techno-Economic Evaluation of Hydrogen-Based Cooking Solutions in Remote African Communities—The Case of Kenya. *Energies* **2023**, *16*, 3242.
158. Pérez-Fortes, M.; Schöneberger, J.C.; Boulamanti, A.; Harrison, G.; Tzimas, E. Formic acid synthesis using CO_2 as raw material: Techno-economic and environmental evaluation and market potential. *Int. J. Hydrogen Energy* **2016**, *41*, 16444–16462. [CrossRef]
159. Rivarolo, M.; Improta, O.; Magistri, L.; Panizza, M.; Barbucci, A. Thermo-economic analysis of a hydrogen production system by sodium borohydride ($NaBH_4$). *Int. J. Hydrogen Energy* **2018**, *43*, 1606–1614. [CrossRef]
160. Zhang, C.; Song, P.; Zhang, Y.; Xiao, L.; Hou, J.; Wang, X. Technical and cost analysis of imported hydrogen based on MCH-TOL hydrogen storage technology. *Int. J. Hydrogen Energy* **2022**, *47*, 27717–27732. [CrossRef]
161. Aadil Rasool, M.; Khalilpour, K.; Rafiee, A.; Karimi, I.; Madlener, R. Evaluation of alternative power-to-chemical pathways for renewable energy exports. *Energy Convers. Manag.* **2023**, *287*, 117010. [CrossRef]